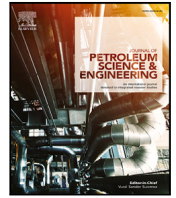




Contents lists available at ScienceDirect

# Journal of Petroleum Science and Engineering

journal homepage: [www.elsevier.com/locate/petrol](http://www.elsevier.com/locate/petrol)

## 4D seismic history matching

Dean S. Oliver<sup>\*</sup>, Kristian Fossum, Tuhin Bhakta, Ivar Sandø, Geir Nævdal, Rolf Johan Lorentzen

NORCE Norwegian Research Centre, Norway

### ARTICLE INFO

#### Keywords:

Time-lapse seismic  
4D seismic  
History matching

### ABSTRACT

Reservoir simulation models are used to forecast future reservoir behavior and to optimally manage reservoir production. These models require specification of hundreds of thousands of parameters, some of which may be determined from measurements along well paths, but the distance between wells can be large and the formations in which oil and gas are found are almost always heterogeneous with many geological complexities so many of the reservoir parameters are poorly constrained by well data. Additional constraints on the values of the parameters are provided by general geologic knowledge, and other constraints are provided by historical measurements of production and injection behavior. This type of information is often not sufficient to identify locations of either currently remaining oil, or to provide accurate forecasts where oil will remain at the end of project life.

The repeated use of surface seismic surveys offers the promise of providing observations of locations of changes in physical properties between wells, thus reducing uncertainty in predictions of future reservoir behavior. Unfortunately, while methodologies for assimilation of 4D seismic data have demonstrated substantial value in synthetic model studies, the application to real fields has not been as successful. In this paper, we review the literature on 4D seismic history matching (SHM), focusing discussions on the aspects of the problem that make it more difficult than the more traditional production history matching. In particular, we discuss the possible choices for seismic attributes that can be used for comparison between observed or modeled attribute to determine the properties of the reservoir and the difficulty of estimating the magnitude of the noise or bias in the data. Depending on the level of matching, the bias may result from errors in the forward modeling, or errors in the inversion. Much of the practical literature has focused on methodologies for reducing the effect of bias or modeling error either through choice of attribute, or by appropriate weighting of data. Applications to field cases appear to have been at least partially successful, although quantitative assessment of the history matches and the improvements in forecast is difficult.

### 1. Introduction

Reservoir simulation models are increasingly used for making forecasts of future reservoir behavior. It is standard practice to calibrate parameters of the simulation model to match production data, as this generally provides greater confidence in the forecast of future production. Unfortunately, production data are available only at widely separated well locations, and the relationship between production data and model parameters is complex. Consequently, seismic data is sometimes acquired to assist in determining fluid movement between well locations. For reservoir monitoring, 4D or time-lapse seismic data are especially useful as they may assist in identifying regions of the reservoir where changes in pressure or fluid content have occurred. Qualitative comparisons between model predictions and actual 4D seismic data are more common than history matching and, when done well, can provide insight into problems with the model (Maleki et al.,

2018). The primary drawback to qualitative comparisons is that the information content in the data is not fully utilized and uncertainty in forecasts is impossible to assess. Despite the potential for increased resolution of model parameter estimates, the use of the 4D seismic data as a further history matching constraint has not yet become standard.

Challenges to the quantitative use of 4D seismic data for reservoir model improvement include the difficulty of assimilating potentially large amounts of data into reservoir models with limited numbers of degrees of freedom, the difficulty of weighting various types of data for simultaneous assimilation, the challenge of choosing parameters capable of matching data while still maintaining plausible distributions of rock properties, prior uncertainty distributions on model parameters that are too narrow, significant errors in forward modeling of seismic data and attributes and large nonlinearity in the relationship between model parameters and data. Fig. 1 illustrates a very high-level

<sup>\*</sup> Corresponding author.

E-mail address: [dean.oliver@norce-research.no](mailto:dean.oliver@norce-research.no) (D.S. Oliver).

<https://doi.org/10.1016/j.petrol.2021.109119>

Received 22 April 2021; Received in revised form 4 June 2021; Accepted 8 June 2021

Available online 19 June 2021

0920-4105/© 2021 The Authors. Published by Elsevier B.V. This is an open access article under the CC BY license (<http://creativecommons.org/licenses/by/4.0/>).

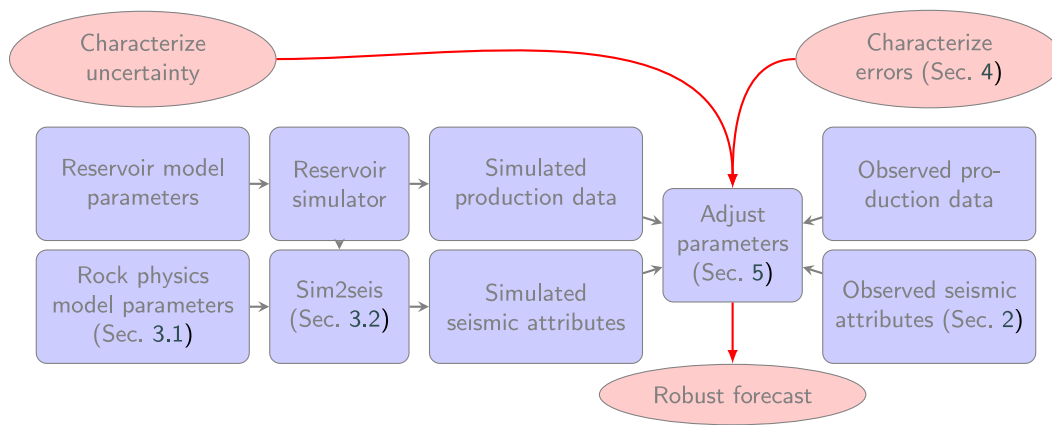


Fig. 1. Generic workflow for seismic history matching.

overview of a general workflow for history matching of production and time-lapse seismic data.

Although history matching of 4D seismic data is difficult even on synthetic “twin” experiments, the application to actual field data has additional challenges, so it has generally been necessary to make a number of simplifying assumptions when history matching real 4D seismic data. These assumptions include (1) the use of relatively small numbers of history matched models to provide estimates of uncertainty in forecasts, (2) qualitative interpretation of data such as interpreted change in oil–water–contact from seismic for assimilation, (3) Gaussian approximations of uncertainty and neglect of scenario uncertainty, (4) neglect of differences in scale between observed seismic data and simulated seismic data, (5) neglect of imperfections in the simulators and neglect of errors in quantification of initial uncertainty in parameters, and (6) neglect of correlations in data error.

The effects of model error appear to be more pronounced in 4D seismic history matching than in traditional history matching of production data because of the additional need for modeling of the seismic attributes from reservoir simulation models (Section 3.2), and because of the volume of data (Section 2). It has been said that “With enough data—and often only a fairly moderate amount—any analyst could reject any model now in use to any desired level of confidence” (Gelman and Shalizi, 2013). Approaches to handling model deficiencies must therefore be an important part of any real-world application of 4D seismic history matching. A consequence of inadequate model assumptions is that the naïve use of Bayes rule for combining information may not improve the model or the forecasts (Vink et al., 2015) and in fact may lead to predictions that are biased and yet overly confident (Brynjarsdóttir and O’Hagan, 2014; Oliver and Alfonso, 2018). An approach that has been advocated in the petroleum industry to avoid the problem of overconfidence in incorrect forecasts is to reduce weight on the data (Sun et al., 2017), but the effect of this action is to possibly ignore important information in the seismic data, simply because it is inconsistent with the prior model. In Section 4.2.3 we review methods for dealing with model error in 4D seismic history matching.

One large potential source of model error in 4D seismic history matching is the petro-elastic model (PEM), which links fluid and reservoir rock properties, such as porosity, saturation, and pressure, to elastic properties such as acoustic velocity and saturated rock density. The PEM is essential for data assimilation of inverted seismic attributes or for forward simulation of seismic amplitudes. In Section 3.1 we review approaches to choosing a PEM for 4D seismic history matching and in Section 3.2 we review methods for simulation of seismic attributes. Algorithms that have been proven useful for dealing with large models and large amounts of data are discussed in Section 5. In Section 6 we provide brief summaries of key field cases that have been discussed in the open literature, focusing on approximations that were required due to the complexity of the case and on the choice

of approach for each case. Although matching of reservoir production data is an important part of seismic history matching, we have largely ignored that aspect of the problem as it has been reviewed fairly recently (Oliver and Chen, 2011).

In a generic inverse problem, one attempts to estimate values of parameters that allow a model to approximately reproduce observed data. In a *seismic reflection inverse problem*, the observations typically consist of pressure amplitudes and the model parameters are typically elastic properties such as density and bulk modulus (Tarantola, 1984) or P-wave velocity, S-wave velocity, and density (Buland and Omre, 2003). The final goal, however, is not simply to estimate elastic properties, but usually to infer reservoir properties such as fluid saturations, porosity and pressure from the observations (Bosch et al., 2010), as these are the properties that determine the amount of hydrocarbons remaining in a reservoir. Hence a second step in the inversion is sometimes applied, in which the rock physics model is used to infer saturation and pressure from density and bulk modulus. If the seismic inversion produces estimates of reservoir properties, then those properties are sometimes referred to as parameters of the model (Landrø and Kvam, 2002), although they may be time varying.

Seismic history matching can be thought of as a type of seismic inversion; that is, one observes seismic amplitudes and from these measurements one attempts to determine the reservoir properties that are consistent with the data. The primary difference between seismic inversion as performed by the geophysicists, and seismic history matching is that, in history matching, physical constraints such as conservation of mass and Darcy’s law are used to restrict the range of plausible distributions of inverted saturation and pressure. In history matching, however, one seldom directly estimates saturations and pressures. Instead, one estimates reservoir properties such as permeability, porosity and fault transmissibilities, then uses these parameters in the model to estimate saturations and pressures. Hence in seismic history matching applications, the term parameter usually refers to reservoir and rock properties that would be input to a reservoir simulator, not to the output of the simulator. In this paper, we sometimes refer to reservoir states such as saturation as a parameter when it is used in the context of seismic inversion.

Regarding the citation of papers: We have attempted to include references to papers that appear to have been influential, based on frequency of citation, but we have also included references that appear to be important based on our assessment of the usefulness of the approach described, or on insight to be gained by discussion of field cases. We have preferentially cited journal papers over conference papers as the journal papers have been peer reviewed and tend to include more information than extended abstracts. We have, however, included many extended abstracts for the simple reason that this method of publication is more common in the geophysical community.

## 2. Data

The major contribution of seismic data, in reservoir characterization, comes in terms of static reservoir model building. The construction of the static reservoir framework relies on reliable geological input. Since no single data type contains sufficient information to accurately characterize the reservoir, there is a benefit from integrating a variety of types of data, such as 4D seismic, well logs, petrophysical, core and production data. 3D seismic data as well as 4D data play a valuable role in the construction of geological models and further in distribution of reservoir properties away from the wells. Seismic data contribute in different stages of reservoir characterization workflows. For example, construction of structural maps of various reservoir formations is carried out by interpreting seismic horizons (Alfi and Hosseini, 2016; Santos et al., 2018). Reservoir facies models are generated by combining the information from seismic, well logs and core data. Seismic attributes such as inverted acoustic impedance are used to constrain the distribution of various reservoir properties (i.e., porosity, net-to-gross ratio, permeability, etc.) geostatistically over the reservoir zones (Bogan et al., 2003). 4D or time-lapse seismic data are sensitive to changes in pressure and saturation within the reservoir, thus potentially helping in identification of fluid flow barriers and reservoir flow properties.

### 2.1. Levels of seismic data integration

For integration of seismic data in history matching workflows, there is a need to define a common domain so that seismic data and simulation results can be compared. In general, 4D seismic observations can be represented in different forms and levels, such as in time or depth, and as seismic amplitudes, impedances or even as pressure and fluid saturation maps. The three main levels for comparison are (1) the seismic level, (2) the elastic parameter level and (3) the simulation model level (see Fig. 2).

In the first level of integration – the seismic domain level – no inversion of seismic data is required, rather observed seismic data are compared directly with simulated seismic data. In this level, a wide variety of data types have been used for history matching including amplitude (Fagervik et al., 2001; Fahimuddin et al., 2010; van Gestel et al., 2011; Skjervheim et al., 2007), time-shift or time-strain (van Gestel et al., 2011; Kjelstadli et al., 2005; Tolstukhin et al., 2012) or amplitude versus angle (AVA) (Luo et al., 2017, 2018a; Soares et al., 2020). AVA data usually provide better insight on reservoir fluid-pressure as well as on lithology and can be effective in complex reservoir scenarios. However, the AVA data tends to be more prone to seismic noise compared to zero-offset seismic data as the AVA is produced using a limited number of seismic traces coming from certain angles. Time-shift and time-strain seismic data are sensitive to porosity, pore-pressure changes inside the reservoirs and are therefore useful for compacting reservoirs like Ekofisk and Vallhall. Although matching at this level avoids the need for inversion, one needs to generate synthetic/simulated data combining seismic modeling with rock physics or petroelastic modeling. The generated synthetic seismic is then compared with observed seismic data (Dadashpour et al., 2008; Luo et al., 2017, 2018a). The forward modeling process can be complex and time consuming, and must be performed each time the reservoir model is changed. Its success depends on the construction of a good PEM and/or sim2seis models as well as the quality of the underlying reservoir or geological models (Section 3).

A cursory review of recent literature indicates that the second level – the elastic parameters level – is the most popular for data integration in 4D seismic history matching. In most cases, acoustic impedance is used as data (e.g., Aanonsen et al., 2003; Gosselin et al., 2003; Roggero et al., 2012; Stephen et al., 2006) as it is generally thought to provide better insight in fluid-pressure changes within reservoirs than seismic amplitude (Maleki et al., 2018; Roggero et al., 2007; Sagitov and Stephen, 2013) and techniques for seismic inversion into impedance data are

widely available. Other data that have been used for history matching at the elastic parameter level include Poisson's ratio (Gosselin et al., 2003), density,  $V_p/V_s$  (Castro et al., 2009) or even ratios of elastic parameters between base and monitors (Alerini et al., 2014; Ayzenberg et al., 2013). These types of data can be equally valuable as acoustic impedance data, however, they are often more noisy and uncertain than the acoustic impedance (Gosselin et al., 2003; Ayzenberg et al., 2013). On the seismic forward modeling side, synthetic impedances or elastic parameters are computed using a petro-elastic model (PEM) that takes saturations and pressures from reservoir flow simulation as inputs (Emerick and Reynolds, 2012; Gosselin et al., 2003; Roggero et al., 2007; Skjervheim et al., 2007). The synthetic elastic parameters from the model are then compared with inverted impedance or elastic parameters, which convert the seismic reflectivity into volumetric property based data that are more suited to cross-domain comparison. Although the need for forward modeling is reduced, data integration in this level is still challenging as the inversion process is inherently more difficult than forward modeling and care must be taken to insure that the inverted results are compared to the modeled results within the seismic frequency bandwidth.

In the third level – the simulation model level – the seismic data are inverted reservoir parameters/states such as maps of pressure and saturation changes (Bhakta et al., 2018; Landrø, 2001). For examples, Zhang and Leeuwenburgh (2017) used saturation maps as data in history matching; whereas Souza et al. (2010) and Park et al. (2015) used both pressure and saturation maps to update reservoir model parameters. These maps or data are then compared directly with simulated outputs. Estimation of these reservoir parameters from seismic data can be obtained either as one-step inversion (e.g., Bhakta, 2018; Bhakta et al., 2020; Landrø, 2001) or as two-step inversion (e.g., Grana and Mukerji, 2015). In two-step inversion, seismic data are first inverted for elastic properties, similar to the situation in the case of second level inversion, then these inverted properties are further inverted for reservoir properties such as pressure and saturation. In one step inversion, seismic data are inverted directly for reservoir properties, where the relationship between amplitude changes and reservoir state changes is approximated directly (Landrø, 2001). One challenge with the use of this approach in data assimilation is the complexity of the uncertainty in the inverted saturation and pressure fields. This level does not, however, require seismic forward modeling for the data comparison.

It is worth mentioning that having a reliable petro-elastic model would always be beneficial for successful data integration irrespective of the level at which the comparison is made. This is because the PEM will be used either on the data side for inversion or on the forward modeling side or on both sides depending on the level of data integration. In most cases, conversion of simulation results into seismic data (for example acoustic impedance) directly in reservoir grid scale is considered as fair practice (Davolio and Schiozer, 2019). However, a better way of data integration should first simulate seismic traces by combining simulation results with PEM and seismic modeling. Then the data integration can be done in any level of our choice as both observed and simulated data will go through same inversion or interpolation procedures. This way of data integration where both simulated and observed data are in an equivalent form can improve the correlation between them and hence improve the applicability of seismic data (Davolio and Schiozer, 2019; Sagitov and Stephen, 2012).

### 2.2. Description of seismic attributes

From seismic data, various attributes can be computed. Selection of an appropriate seismic attribute can be instrumental in a successful history match. Seismic attributes potentially contain a large amount of information that is not available from production data. However, not all seismic attributes are sensitive to all reservoir properties, thus there is a need to identify the most useful. For example, the time-shift

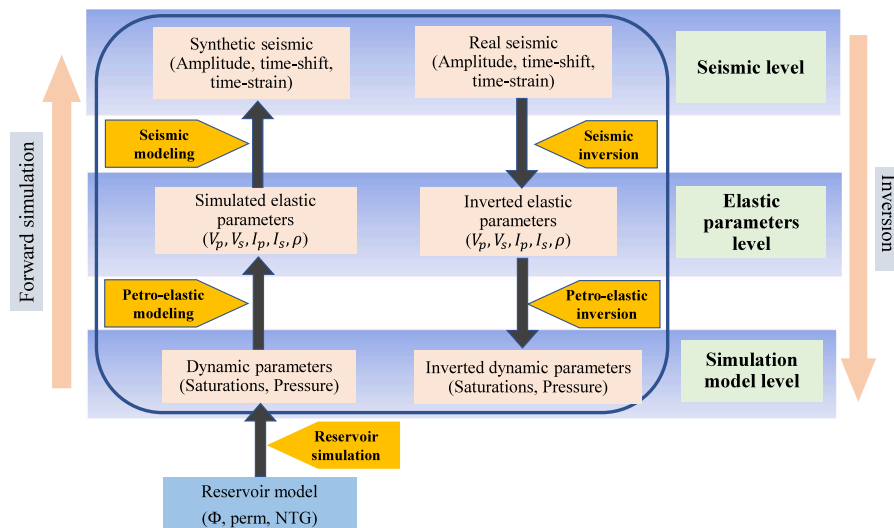


Fig. 2. The various levels of seismic data integration.

attribute is good for detecting pressure changes, whereas amplitude or impedance changes are better suited for detecting saturation changes. Further, a producing field can have a variety of distinct production related effects that can be decoupled/distinguished if several attributes with different sensitivity are available for assimilation. Selection of one or more attributes for history matching should be based on a pre-sensitivity analysis to decide how dynamic changes effect the potential attributes. Extraction of a proper attribute depends on other factors too, for example, increase of precision of the extracted attribute escalates both the demand for computational power as well as the complexity of the seismic analysis (Jin et al., 2012b). The potential of the extracted attributes is partially dependent on the goodness of corresponding simulated attributes, thus on seismic and rock physics forward modeling. However, this forward modeling process is often time consuming and complex in nature (Obidegwu et al., 2017). Therefore, deciding on attributes is somewhat constrained by the availability of forward seismic modeling. In the following sections, we will discuss various attributes that are used in seismic history matching.

### 2.2.1. Conventional seismic attributes

Surface and volume attributes are the two most used seismic attribute types in seismic history matching. They are extracted or computed over various reservoir horizons or over reservoir volumes.

**Maps** One of the most common and robust attributes in seismic history matching is map or surface based. Attribute maps can be generated along an interpreted horizon or by averaging several layers or horizons. Map-based attributes are less susceptible to data noise than volume-based attributes as the mapped attribute is usually computed over a time-window. However, there is a trade-off between the resolution and robustness of the attribute when choosing the width of the window. A long time window results in less noise, but lowers the resolution, i.e., it does not contain any vertical information, unless multiple maps are used.

Various approaches are used to extract the maps. For example, time-horizons from top, base and/or intra-reservoir boundaries can be extracted as 4D maps (Kazemi and Stephen, 2012; Stephen et al., 2009; Waggoner et al., 2003). Further a map of root-mean-square (RMS) amplitude generated over a time-window or whole reservoir zone can be used in data integration (Souza et al., 2018; Stephen et al., 2006; Stephen and MacBeth, 2008). The map can be extracted from various types of data such as seismic amplitude, time-shift, time-strain data (Fagervik et al., 2001; van Gestel et al., 2011) or from inverted seismic data such as acoustic impedance (Emerick, 2016). Even maps

of saturation or pressure can be used as seismic attributes. van Gestel et al. (2011) extracted attribute maps of both seismic amplitude and time-shift using 4D processed life of field seismic surveys of the Valhall field. In that study, the time-shift attribute was converted into observed compaction maps for comparison with simulated compaction. Another way of using seismic amplitude is by summing negative amplitudes (SNA) over a reservoir formation interval (Briceño, 2017; Côte et al., 2020; Geng et al., 2017). The rationale for the use of only negative parts of the seismic signal is that, usually, a porous reservoir is acoustically softer than the background formation. The changes of SNA values from base seismic data indicate changes in fluid-pressure distribution due to production or injection within reservoirs.

**Cubes** Another common way to assimilate seismic data is by using volume or cube attributes (Lorentzen et al., 2020, 2019; Luo et al., 2018a). Volume attributes can be computed in the time or depth domain and/or seismic or reservoir grid domain. For example, Luo et al. (2018a) and Soares et al. (2020, 2019) use volume of amplitude versus angle (AVA) seismic data in time. Whereas, Alfonzo and Oliver (2019) and Lorentzen et al. (2020, 2019) use volume of acoustic impedance data in depth where the acoustic impedance are interpolated/upscaled for comparison on the reservoir grid. Usually seismic data have lower vertical resolution than the reservoir model layer thicknesses. Therefore, generating or interpolating seismic attributes for each reservoir grid cell does not increase the information content.

### 2.2.2. Additional seismic attributes

We will discuss in Sections 3.1 and 3.2 the process of building a realistic forward model, including both seismic and petro-elastic modeling. The modeling of seismic attributes is typically complex and expensive and many of the parameters of the models are poorly constrained. Therefore, simpler alternatives have been proposed as an alternative to full modeling, for example, fluid fronts (Leeuwenburgh and Arts, 2014; Trani et al., 2012) and binary image-based attributes (e.g., Jin et al., 2012a,b; Obidegwu et al., 2017; Tillier et al., 2013). The details of these alternative attributes are discussed below.

**Fluid front** Interpretation and parameterization of seismic information in terms of front propagation can be considered as a seismic attribute (Leeuwenburgh and Arts, 2014; Mannseth and Fossum, 2018; Zhang and Leeuwenburgh, 2017). The technique was first introduced by Kretz et al. (2004) based on streamline simulation and applied in simple 2D cases. The method was further developed and implemented for conventional finite-difference reservoir simulators and in the ensemble-based data assimilation context by Trani et al. (2012),

where they parameterized inverted saturation data in terms of front arrival times. However, there is a potential drawback of using travel times as it requires at least twice as long simulation run time for accurate ensemble arrival time predictions (Trani et al., 2017). This shortcoming can be addressed by parametrizing the seismic data in terms of front positions (Leeuwenburgh and Arts, 2014). Different types of seismic data (i.e., seismic amplitude maps, inverted acoustic impedance or saturations from reservoir grid cells) can be used for the parameterization. In many cases, the front attribute is extracted directly from seismic amplitude, which avoids the necessity of seismic inversion. The assumption that the observed seismic amplitude front can be compared with the saturation front requires that other effects are negligible, including for example the effect of pressure variation or compaction, the effect of variation in porosity or net-to-gross ratio. If trends in these quantities are, in fact, important, then the results of a direct comparison will be biased. Leeuwenburgh et al. (2016) discuss how different seismic interpretations can be equally plausible for the same time-lapse amplitude maps due to various factors such as a different seismic processing sequence and understanding of the seismic signal, poor quality of the data or using various threshold values, and thus lessens the efficacy of the method to a great extent.

**Binary images** A closely related approach to avoid the forward modeling part in history matching is to use a binary image as an attribute (Jin et al., 2012a,b; Obidegwu et al., 2017). In this approach, first 4D seismic data or anomalies are interpreted and clustered into ‘hardening’ and ‘softening’ signals (Obidegwu et al., 2017) and then further converted into binary maps (Chassagne et al., 2016). The attribute contains mostly first order information from 4D seismic data, thus it provides a quick and effective way to integrate the most obvious information (Jin et al., 2012b). The binary map attribute can be seen as a reduction of level of information into two states (0 and 1). Thus the success of extracting proper binary images, i.e., selecting of the zones, requires interpretation of the 4D seismic response associated with the dynamic changes in the reservoir (Jin et al., 2012b) and results will depend on the threshold selection. Jin et al. (2012b) converted flooded-zone pattern derived from 4D seismic data into binary images, whereas, Chassagne et al. (2016) converted seismic information to binary gas maps by interpreting various reservoir processes like gas expansion, dissolution and displacement. Obidegwu et al. (2017) extracted binary (water and gas) maps by interpreting and deciphering potential gas and water signals due to the injector/producer location. Recent work from Davolio and Schiozer (2018) shows computation of binary maps by clustering high and low pressurized zone from seismic data.

**Onset time** The onset time attribute for seismic data, introduced by Vasco et al. (2014), is defined as the calendar time when changes in time-lapse data crosses a pre-specified threshold value at a given location (Vasco et al., 2015). Therefore, the attribute is generated by collapsing multiple seismic surveys into a single map of changes propagating in the reservoir (Hetz et al., 2017). The threshold value is crucial to compute the onset time attribute and itself depends on the signal-to-noise ratio of seismic data as well as on the reservoir state that is being tracked (e.g. saturation front and/or pressure front). The main advantages of this attribute is the ability of substantial data reduction. Therefore, this approach becomes a computationally efficient method to integrate frequent time-lapse seismic surveys (Hetz et al., 2017). Further, the attribute is not very sensitive to the choice of petro-elastic models, but rather strongly sensitive to fluid-pressure changes within the formation (Vasco et al., 2014). Hetz et al. (2017) showed the applicability of this attribute to estimate permeability variation between boreholes in a CO<sub>2</sub> monitor site. The attribute was used for a heavy oil reservoir in the Peace River Field, Canada, where daily time-lapse seismic surveys are recorded by the permanently buried seismic monitoring system to monitor the steam injection process. However, implementation of this attribute becomes less promising in most of the

producing fields due to the fact that less frequent seismic surveys may not have sufficient information to resolve and build the onset time map. Even interpolation of the attribute will not benefit for highly infrequent seismic surveys as dominant underlying physics might not be captured by the seismic surveys, for example shifting from saturation dominated case to pressure and/or temperature dominated case (Liu et al., 2020).

**Well2seis attribute** Another efficient way of integrating frequently acquired seismic data is to use the ‘well2seis’ attribute. In this approach, the large volumes of seismic data coming from several repeated surveys is condensed into a single attribute (Yin et al., 2019). The attribute is extracted by defining a linear relationship between 4D seismic responses and the cumulative changes of reservoir fluid volumes derived from wells (Yin et al., 2015, 2019). The attribute has been applied in various North Sea reservoir scenarios (Yin et al., 2015, 2019). However, there are a couple of challenges for successful application of the attribute. To obtain a statistically significant estimate of the well2seis attribute, at least four seismic surveys are required (Yin et al., 2019). Further, proponents state that a clear understanding of the communication and connectivity between wells and the similarity of the well behavior is the fundamental prerequisite for the success. This, however, is the objective of history matching.

As mentioned above 3D and 4D seismic data may contain large amount of valuable information. However, optimal information extraction depends on many factors coming from seismic acquisition, processing and inversion of seismic data. Therefore, proper filtering, time-shift correction and frequency matching are required prior to the extraction of different attributes. In addition, the data must be properly calibrated and normalized to match quantitatively with model predictions (Kazemi et al., 2011). Proper scaling (upscaling and/or downscaling) is required before comparing with the modeled response (Kazemi and Stephen, 2012; Stephen and Kazemi, 2014). Further, time-to-depth conversion of data and quantification of both 3D and 4D noise play a very crucial role in successful seismic data integration.

### 2.3 Summary

- Seismic data is often complementary to other types of reservoir data, and thus is potentially beneficial. Optimal value extraction of seismic data depends on various factors, such as availability of inversion or forward modeling tools and low noise levels on the data.
- Various types of seismic data coming from different levels can be assimilated. However, recent trend indicates that the second level – the elastic parameters level – and specially acoustic impedance data is the most popular for data integration in 4D seismic history matching due to its relatively low computational cost, straightforwardness of data interpretation and cross-domain comparison.
- Map or volume based seismic attributes are common to be used in history matching. These types of attribute require a PEM and/or simulator-to-seismic tool to be in place for data comparison either for seismic inversion or for forward modeling or for both. As there is always a challenge to simulate corresponding attributes due to the lack of proper seismic and petro-elastic model, other attributes like displacement front, binary images are being introduced.

## 3 Forward modeling

### 3.1 Petro-elastic models (PEM)

Application of seismic forward modeling in reservoir characterization and exploration projects has been common for several decades. As 3D and 4D seismic data started to be used actively to evaluate and update reservoir models, the need for producing realistic seismic forward modeling based on geo- and reservoir simulation models

(sim2seis) increased. The objective of sim2seis is to produce synthetic seismic data to compare with real seismic observations and apply the mismatch in either manual or automatic updating of critical reservoir model parameters. There are several challenges related to computation of realistic synthetic seismic data from the simulation models. The simulation models are constructed to give optimal modeling and prediction of the fluid flow and are not specifically designed for forward seismic modeling. Seismic modeling needs seismic velocities and densities in a complete 3D volume including the reservoir zones and also parts of the over-and underburden and of non-reservoir zones, all of which are missing from typical reservoir simulation models.

Construction of a 3D velocity model suitable for seismic modeling relies on petro-elastic models (PEM) that convert fluid and static rock properties to elastic parameters. In addition, for use in 4D work, the PEMs should include a fluid substitution model and a model for pressure sensitivity. The PEM constitutes the most important building block in the sim2seis process.

Amini (2014) gives a thorough review of PEM construction for sim2seis workflows. This includes guidelines to construct PEMs suitable for use in history matching projects. Mavko et al. (2009) and Grana et al. (2021) provide comprehensive reviews of the underlying rock physics models used. In Fig. 3, a simplified workflow for construction of PEM is presented. The basic equations for calculating seismic velocities from elastic parameters are

$$V_p = \sqrt{\frac{K_{\text{sat}} + \frac{4}{3}\mu_{\text{sat}}}{\rho_{\text{sat}}}} \quad \text{and} \quad V_s = \sqrt{\frac{\mu_{\text{sat}}}{\rho_{\text{sat}}}} \quad (1)$$

where  $K_{\text{sat}}$ ,  $\mu_{\text{sat}}$  and  $\rho_{\text{sat}}$  are the bulk modulus, shear modulus and density of the saturated medium, respectively.  $V_p$  and  $V_s$  are P-wave and S-wave velocities. They are the velocities related to compressional and shear waves propagation, respectively.

The most common model for estimating the effect of saturation changes on the elastic parameters is the Gassmann fluid substitution law (Gassmann, 1951):

$$K_{\text{sat}} = K_{\text{dry}} + \frac{(1 - \frac{K_{\text{dry}}}{K_s})^2}{\frac{\phi}{K_f} + \frac{1-\phi}{K_s} - \frac{K_{\text{dry}}}{K_s^2}} \quad \text{and} \quad \mu_{\text{sat}} = \mu_{\text{dry}} \quad (2)$$

where  $K_{\text{dry}}$ ,  $\mu_{\text{dry}}$ ,  $K_f$ ,  $\phi$  are dry frame bulk modulus, dry frame shear modulus, effective fluid bulk modulus of the fluid mixture, and porosity, respectively.  $K_s$  is the bulk modulus of the mineral constituting the matrix. The effective fluid bulk modulus and density can be calculated using the equations given by Batzle and Wang (1992).

Estimation of the matrix bulk modulus,  $K_s$ , is based on the fractions of minerals constituting the rock. Most applications are based on averaging of the Hashin–Shtrikman upper and lower bounds (Hashin and Shtrikman, 1963) or the Voigt–Reuss–Hill average (Hill, 1963) (arithmetic mean of Voigt (1929) as upper and Reuss (1929) as lower bounds).  $K_f$  can be calculated similarly using the Voigt–Reuss–Hill average.  $\rho_f$  can be computed by averaging the volume fraction and density of each fluid phase in the pores.

$K_{\text{dry}}$  can be estimated from lab measurements on core samples. Alternatively, it is possible to use Eq. (1) with velocity and density measurements from relevant well logs to estimate  $K_{\text{sat}}$  at the well log scale. Then  $K_{\text{dry}}$  can be estimated by a simple rewriting of the Gassmann equation (Eq. (2)). Empirical equations for  $K_{\text{dry}}$  and  $\mu_{\text{dry}}$  are normally obtained in 4D projects by assuming a polynomial dependence on porosity. Often polynomial regression curves of the form

$$K_{\text{dry}} = K_s(a\phi^2 - b\phi + c) \quad \text{and} \quad \mu_{\text{dry}} = \mu_s(d\phi^2 - e\phi + f)$$

are used (Briceño, 2017) where  $K_s$  and  $\mu_s$  are the effective matrix moduli, respectively.

In addition to porosity and mineral dependency, effective stress sensitivity should also be explicitly introduced in the determination

of  $K_{\text{dry}}$ . The prediction of stress sensitivity is often based on the Hertz–Mindlin contact model:

$$K_{\text{dry}} = \sqrt[3]{\frac{C^2(1-\phi)^2\mu_s^2}{18\pi^2(1-\nu_s)^2} P_{\text{eff}}} \quad \text{and} \quad (3)$$

$$\mu_{\text{dry}} = \frac{5-4\nu_s}{5(2-\nu_s)} \sqrt[3]{\frac{3C^2(1-\phi)^2\mu_s^2}{2\pi^2(1-\nu_s)^2} P_{\text{eff}}}$$

where  $C$  is the average number of contacts per grain,  $\mu_s$  and  $\nu_s$  are the shear modulus and Poisson's ratio of the solid grains and  $P_{\text{eff}}$  is the effective stress.

Considering two different effective stress states in Eq. (3),  $P_{\text{eff}}^i$  at the initial reservoir state and  $P_{\text{eff}}^t$  at a given production time  $t$ , we find a simple relation between the bulk moduli and effective stress:

$$\frac{K_{\text{dry}}(t)}{K_{\text{eff}}^i} = \left( \frac{P_{\text{eff}}(t)}{P_{\text{eff}}^i} \right)^{\frac{1}{3}}$$

and similarly for the shear moduli. In practice, the exponent will differ from  $\frac{1}{3}$  and needs to be calibrated using ultrasonic core measurements, thus the relationship becomes

$$\frac{K_{\text{dry}}(t)}{K_{\text{eff}}^i} = \left( \frac{P_{\text{eff}}(t)}{P_{\text{eff}}^i} \right)^{h_k}$$

where  $h_k$  is referred to as the Hertz coefficient. Having established  $K_{\text{eff}}^i$  and  $\mu_{\text{eff}}^i$  values for the initial state, this gives us the pressure dependency of the moduli that is now calibrated to the ultrasonic core measurements and can be used in the Gassmann equation (Eq. (2)) and finally in Eq. (1) to find the velocities in the saturated states with pressure sensitivity included.

Although the formulas for the PEM may seem to be straightforward, challenges are frequently reported in the application of the PEMs in sim2seis work. The PEMs are relations transforming the fine-scaled (core, log scale) static and dynamic properties to elastic parameters. To be useful in sim2seis applications, they need to be upscaled from the fine scale to the simulation grid scale and calibrated to field observations at the seismic scale. This is a non-trivial exercise as the fine-scaled PEM is lithology and rock fabric specific, while at the simulator grid scale, these effects are mixed. Thus, the effect of assumptions introduced in the PEM calibration and upscaling process, especially related to handling of sub-seismic heterogeneities in real reservoir settings should be understood and described. Also, since the simulators typically use cut-offs to porosity and  $V_{\text{clay}}$  when upscaling from the geomodel to the reservoir model, this has to be handled when the fine scale PEM is upscaled to the coarse reservoir model. An important aspect of this problem is the handling of sand/shale sequences (Avseth et al., 2006).  $K_{\text{dry}}$  is determined as a function of porosities from the zero porosity mineral point to critical porosity by using modified Hashin–Shtrikman bounds. Thus, a consistent variation of  $K_{\text{dry}}$  going from the net sand parts to the non-reservoir shaly parts is established. Falcone et al. (2004) described a methodology for selecting a scale dependent PEM in 4D SHM and demonstrated the proposed workflow on a field case. Menezes and Gosselin (2006) developed a methodology for selection of upscaled PEMs based on the fine scale PEMs through an optimization procedure in the calibration of the dry rock parameters at reservoir scale. In the procedure they used upscaled impedances based on the log scale PEM as the 'observed' data and the parameters based on the upscaled PEM as 'predicted' data.

A potential solution to the problem of selecting the optimal number of PEMs and selecting the minimum vertical grid size in the flow model to obtain satisfactory match with seismic observations has been described by Alfred et al. (2008) while Amini (2014) emphasized the challenges involved with the use of an upscaled PEM in sim2seis workflows. When choosing the coarser scale, it is important to perform sensitivity analyses to determine the acceptable degree of coarsening by setting a limit on the degree of preservation of the seismic modeling response from the upscaled model. This is a crucial step in successful

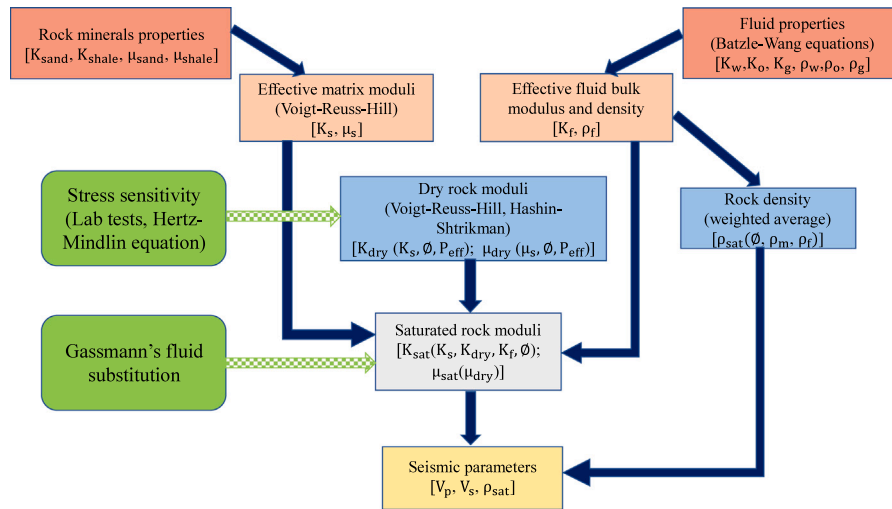


**Fig. 3.** The workflow of a petro-elastic (PEM) model. The PEM workflow starts by using the individual rock minerals and fluid properties to determine the effective matrix and fluid moduli, respectively. Then the dry rock moduli are determined as a function of porosity and pressure. Further, saturated rock density is calculated using porosity and fluid saturations as input. The saturated rock moduli are then determined using the Gassman fluid substitution law. Finally, the seismic parameters are calculated using the saturated moduli and rock density. In the 4D PEM, it is necessary to include fluid and stress sensitivity as shown in the green boxes.

field application, but one that is not often described in the published literature.

There are also normally large uncertainties related to the stress sensitivity models for elastic moduli. One main challenge is that properties estimated from measurements made on cores at ultrasonic frequencies are often not representative of properties to be used at reservoir simulation scale. There are always heterogeneities (faults, fractures, inhomogeneities ...) between core scale and the coarser simulator scale that complicate the prediction of effective velocities at reservoir grid and seismic scale. In addition, the coring process itself and the change in stress tend to introduce changes to the core, making the estimates of properties less reliable. Finally, there are dispersion effects that can make the ultrasonic measurements (at Mhz frequencies) not representative at seismic frequencies (5–100 Hz). These challenges are well-known in the geophysical community and methods to assess the reservoir stress sensitivity have been discussed in the literature. Nes et al. (2002) gives a thorough description of the challenges related to application of ultrasonic core measurements in 4D seismic studies, focusing on core representativity issues and effects of core damage on measured velocities. Landrø and Kvam (2002) used real field 4D data sets combined with the Hertz–Mindlin theory to develop equations to quantify overpressure from multiple 4D seismic surveys.

MacBeth (2004) developed a formulation to capture the effect of core weakness by introducing the concept of *excess of compliance*, leading to the formulae

$$K_{\text{dry}} = \frac{K_{\infty}}{1 + E_k e^{-\frac{P_{\text{eff}}}{P_k}}} \quad \text{and} \quad \mu_{\text{dry}} = \frac{\mu_{\infty}}{1 + E_{\mu} e^{-\frac{P_{\text{eff}}}{P_{\mu}}}}$$

where  $K_{\infty}$  and  $\mu_{\infty}$  are the background, high-pressure asymptotes,  $E_k$ ,  $P_k$ ,  $E_{\mu}$  and  $P_{\mu}$  are rock stress sensitivity constants from available core measurements that define the shape of the stress sensitivity curve. Avseth and Skjei (2011) and Avseth et al. (2016) also consider core measurements to be too unreliable to directly establish stress sensitivities. They develop a methodology for prediction of stress sensitivity in patchy cemented sandstones based on a Hashin–Shtrikman approach combined with contact theory. The method has been applied to the prediction of observed 4D time shifts in a real field case from the North Sea. One important parameter in the study is the degree of cementation in the sandstones — even a few percent cementation is shown to give large impact on the stress sensitivity. Omofoma and MacBeth (2016) use 4D seismic data to establish the stress sensitivity. They analyze 4D amplitudes from several repeated surveys in areas where

the 4D response was believed to be due to pressure changes. From this, empirical relations were established that were used in quantifying 4D pressure effects in several field cases.

Acquisition of repeated sonic logs in producing or dedicated observation wells would increase the confidence in the stress sensitivity and 4D fluid substitution models used, but these are hard to acquire due to cost and operational issues (Falcone et al., 2004). Proper calibration data for the stress sensitivity and fluid substitution effects are believed to have the highest improvement potential in PEM construction in 4D applications.

As a consequence of the challenges related to establishment of reliable PEMs for history matching projects and to avoid the complexities in running a complete sim2seis as part of the SHM process, the use of proxies to the PEM have been proposed. MacBeth et al. (2016) introduced a proxy that links the 4D seismic attribute change ( $\Delta A$ ) to production related changes (pressure and saturations) by a second order Taylor series expansion:

$$\Delta A = (a_1 \Delta P + a_2 \Delta S_w + a_3 \Delta S_g + a_4 \Delta P^2 + a_5 \Delta S_w^2 + a_6 \Delta S_g^2 + a_7 \Delta P \Delta S_w + a_8 \Delta P \Delta S_g + a_9 \Delta S_w \Delta S_g) A_0$$

where  $A_0$  is the attribute computed from the reference dataset.  $\Delta P$ ,  $\Delta S_w$ ,  $\Delta S_g$  are changes in pore-pressure, water saturation and gas saturation, respectively. The coefficients are constant over the area of interest. The proxy is thus limited to areas/volumes with small variations in the static PEM parameters. The proxy facilitates the integration of 4D data in the history matching loop.  $A_0$  can in principle be any seismic attribute, for robustness it is recommended to use differences of 3D maps as the 4D attribute. The maps are preferably linked to a time window around a clear, stable horizon. Often the top reservoir horizon is a natural choice. The method is applied and compared with the use of a complete PEM and sim2seis modeling in a 4D SHM loop giving satisfactory results for two synthetic datasets. Danaei et al. (2020) uses a simplified version of MacBeth's proxy:

$$\Delta A = a \Delta S_w + b \Delta P$$

keeping only the linear part linking water saturation and pressure changes to 4D acoustic impedance changes ( $\Delta A$ ). The method is applied to ensemble based data assimilation on a synthetic case based on an oil field in the Campos basin and compared with the use of the full petro-elastic models. Their conclusion is that the PEM proxy gives promising results, especially in reproducing the past reservoir behavior, while data assimilation with the complete PEM gave more reliable future forecasts.

### 3.2 Sim2seis

The upscaled and calibrated PEM (normally, several PEMs are used depending on lithofacies) are applied to the static and dynamic values in each active cell of the reservoir model, giving the seismic velocities and densities needed for seismic simulation. In each cell, the NTG is normally used to separate models for the sandy and shaly parts. The majority of reported field cases in 4D SHM do the integration of seismic data in the history matching loop by comparing seismic inversion results in terms of acoustic impedance with the simulated impedance ( $I_p = \rho V_p$ ) calculated from the PEM in the reservoir model domain. This requires a time/depth conversion, horizontal upscaling and resampling to the reservoir grid of the seismically derived impedance cube. However, no sim2seis computation is typically performed in this approach other than possible vertical band-pass filtering of the synthetic impedance cube to account for the frequency differences between observed and synthetic impedances (Alfonzo and Oliver, 2019; Emami Niri and Lumley, 2015). Alternatively, the synthetic impedances are areally downscaled to the seismic grid by interpolation techniques (Stephen et al., 2006); and the matching performed at the seismic bin domain. Enchery et al. (2007) suggest to downscale pressure and saturation values from the coarse reservoir grid to a finer grid in targeted smaller downscale areas by performing new fluid flow calculations on the finer grid. The resulting values are then used as input to sim2seis and compared to seismic attributes at the seismic bin scale.

To perform a complete sim2seis, we need to supply seismic parameters also in the non-active cells. The seismic response is dependent on acoustic contrasts not only between active cells, but just as importantly on the acoustic contrast between reservoir and non-reservoir units. Thus, the non-active cells and units must be filled with elastic parameters derived from relevant well logs. Similarly, parts of the over- and underburden must also be included, covering a length more than one seismic wavelength, to ensure capture of the seismic reflections at top and base reservoir and possible tuning effects from layers directly above and below the reservoir. To precondition the completely populated 3D reservoir model to a seismic modeling grid, seismic velocities and densities have to be interpolated to the regular Cartesian seismic grid. The choice of modeling algorithm is not much discussed in the literature, although a comparison of different approaches is given in Amini et al. (2020). It is shown there that for the considered field case, the 1-D convolution method gives satisfactory results compared to a complete 2D pre-stack elastic finite difference simulation. This means that the effects of internal multiples, mode conversions and transmission are of secondary order. As 4D SHM using sim2seis may require a huge number of seismic simulations, it is mandatory to apply efficient modeling algorithms. The degree of complexity needed in the seismic modeling depends on the selected 4D attributes. As mentioned, using seismic inversion results as the seismic observations does not, in principle, require seismic forward modeling. However, consistency between the synthetic seismic data based on the 3D initial static model and the pre-production 3D seismic data is important to avoid possible divergence in the history matching loop (Emami Niri and Lumley, 2015). Also, Sagitov and Stephen (2012) demonstrated the need to match predicted and observed data using the sim2seis output in the prediction step. This is exemplified in a field case where observed data are in the form of RMS maps of colored inversion (pseudo-impedance) results. It is shown that the SHM results improve when the misfit function is based on predicted pseudo-impedances estimated from the synthetic seismic sections using the sim2seis process rather than using impedance values calculated directly from the PEM.

### 3.3 Reservoir flow simulation

The sim2seis procedure requires input of dynamical quantities describing the state of the petroleum reservoir. The dynamic modeling is

performed by the reservoir simulation model. Here, the partial differential equations describing the fluid-flow are solved on a numerical grid. In most cases, the unknowns are the saturation and pressure values in all grid cells. The solution at a given time-step can then be utilized in the sim2seis calculation, or to predict relevant production/injection values at the wells. Reservoir flow simulation is a large topic, and a comprehensive review of this topic is outside the scope of this work. We will refer to Aziz and Settari (1979), Chen et al. (2006) and Peaceman (1977) for more information regarding the topic. In the following, we focus on the issues that are relevant for 4D seismic modeling.

#### 3.3.1 Saturation and pressure

In a petroleum reservoir, there exists a range of different chemical components, both in the fluid phase and in the gas phase. A standard procedure is to assume that the reservoir fluid consist of three components: water, oil and gas in a three-phase system. The interaction between the oil phase, the gas phase and the water phase can then be modeled numerically always keeping the mass balance preserved. This modeling setup is denoted a black oil simulator. There are, however, some cases where it is necessary to model the individual chemical components. Preserving the mass balance of each component, the interaction between the components in the different phases are modeled numerically. This modeling setup is denoted compositional simulation. For applications of 4D seismic history matching, this approach might be necessary in certain cases, for instance those involving CO<sub>2</sub>, e.g., Eydinov et al. (2008), Hosseinioosheri et al. (2018), Leeuwenburgh et al. (2016), Ouenes et al. (2010), Pamukcu et al. (2011), Shi et al. (2019) and Singh et al. (2010).

#### 3.3.2 Compaction

Compaction is an important driving force in many petroleum reservoirs, and can be caused by, e.g., pressure reduction, or water-weakening associated with water injection. The latter effect is most prominent in carbonate reservoirs. For the Ekofisk field, 4D seismic analysis helps to perform reservoir compaction mapping (Smith et al., 2002). Here, seismic compaction maps were generated by comparing seismic travel time changes between seismic surveys. This information was used to manually tune the reservoir model. Moreover, the 4D seismic signal was used to develop a geocellular model to properly account for the reservoir compaction. In Tolstukhin et al. (2012) a computer-assisted history matching process was considered. In the forecast stage, compaction of the reservoir is modeled using an in-house flow simulator and a geomechanical model. In a study of the Valhall field (Han et al., 2013), a geomechanical model was coupled with the flow simulator. For every numerical time step, when the flow simulator has produced a new pressure field, the geomechanical model computes the stress and strain response in three dimensions with corresponding changes in compressibility, porosity and permeability. The improved simulation results were utilized to model the reservoir compaction. Here, the model was validated using 4D seismic. Furthermore, the coupled model provided a better match to the observed production data. However, no history matching was done.

#### 3.3.3 Temperature

Accurate temperature modeling is important for many applications, such as Steam Assisted Gravity Drainage (SAGD), in situ combustion, and CO<sub>2</sub> injection. In Hiebert et al. (2013), a thermal simulator was used to model the effect of temperature on changes in the volume of the steam chamber for history matching of 4D seismic data in a SAGD setup. The paper showed that changes in the steam chamber size gave a large seismic response. Depending on the gas saturation and temperature, a simulation block was determined to be part of the chamber, or not, leading to a binary map used as seismic data. Following this approach, a simulation chamber was produced, which again was compared with the measured 3D shape of the chamber, derived from the measured seismic data. In Lerat et al. (2009) the added

value of 4D seismic data in the context of SAGD was demonstrated. In addition to the thermal evolution, the geomechanical effects were modeled by coupling the flow simulator and the geomechanical simulator. The study was performed on a field located in the Athabasca oil sands. Unfortunately, neither seismic nor observation well data was available for history matching. Another coupling of the flow simulator and geomechanical simulator for a SAGD application was reported in Gu et al. (2011). A history match was performed in which measured fluid rates, cumulative fluid volumes, temperatures, pressures and steam quality at the injection/production wells; temperature, pressure, deformation, and microseismic events measured at observation-well or at the surface; and 4D seismic data were all utilized. The authors claim that coupled simulation and history matching should be repeated until a satisfactory match is obtained. The paper does not consider automation of the history-matching process, and there is no method for evaluating the quality of the history match.

The movement of a thermal front during an in situ combustion procedure has been investigated by Vedanti and Sen (2009). The paper showed that the thermal front could be detected from 4D seismic measurements. However, no history matching, or modeling was performed in this paper. Moreover, to our knowledge, there has not been any in situ combustion applications where 4D seismic data is used for history matching.

Finally, thermal modeling is often necessary for CO<sub>2</sub> applications. In Zhang et al. (2014), studying Layer 9 in the Sleipner field model, an approximate match with the observed CO<sub>2</sub> plume was achieved by introducing lateral permeability anisotropy coupled with either an increased reservoir temperature with CH<sub>4</sub> impurities in the CO<sub>2</sub> stream or a second feeder from the deeper layers. The study used a comprehensive publicly accessible data-set for the Sleipner field, including six 4D seismic surveys and well log data. The paper does not provide details regarding the model calibration procedure, and the evaluation of the calibrated model is done by visually comparing the simulation results with the inverted seismic data. Another application with coupled thermal and rock-mechanical simulation is given in Shokri et al. (2019) for cold injection of CO<sub>2</sub>. In this paper, 3D seismic data was utilized initial characterization of geology but not for history matching.

### 3.4 Summary

A reliable forward modeling of seismic attributes in SHM is critical to take advantage of high quality 4D data. The most important factors in the forward modeling part of the SHM workflow are :

- Calibration and optimal upscaling of the PEM. The upscaling should use conservation of the seismic response as guideline (Amini, 2014). If the final PEM is considered too uncertain to be used in the HM workflow, a proxy model could be evaluated (MacBeth et al., 2016).
- The simulation of the 4D baseline seismic data from the static reservoir model should be consistent with the structural 3D seismic interpretation. Parameters in the static model should be conditioned on 3D seismic data prior to quantitative 4D SHM. (Emami Niri and Lumley, 2015; Stephen et al., 2006).
- The observed 4D attributes used in the HM workflow should preferably be matched to synthetic versions of the same attributes computed from the output from a full sim2seis workflow (Sagitov and Stephen, 2012).
- Application of an efficient, fit-for purpose seismic modeling technique (Amini et al., 2020). The need for advanced applications (visco-elastic, anisotropic, 3D FD modeling) should be documented through an upfront modeling study due to their large impact on simulation run time.
- The field of numerical reservoir simulation has the necessary maturity to model a wide range of complex reservoir physics. The literature shows that many unconventional recovery techniques also provides a substantial 4D signal. Hence, the 4D signal also has potential for history matching in complex reservoir settings.

## 4 Weighting data

When any type of data assimilation is performed, there is a need to integrate information from a variety of sources. In time-lapse seismic history matching it is common to combine information from repeated seismic surveys, production and injections wells, cores, well logs, PVT analysis of fluids, and analog outcrops. When the measurements to be assimilated are noisy and the models are imperfect, information from various sources may appear to be in conflict. Additionally, if the parameters in a model are physically motivated, information in the data may be in conflict with prior estimates of model parameters or with physical constraints (e.g. porosity between 0 and 1).

In all practical applications of history matching, the parameters of a model of the physical system are adjusted in such a way that the misfit between observed data and simulated data is minimized, while attempting to keep values of the parameters in the plausible range (Oliver and Chen, 2011). The misfit is usually defined through a total objective function that is the sum of two terms: one that measures the misfit between the observed data and the simulated data and another that measures the difference between the history matched model and the best estimate of model parameters prior to history matching. When the objective function is minimized and the value of the objective function is sufficiently small, the model is said to be history matched.

### 4.1 Objective function

The most common objective function used for seismic history matching is obtained from Bayes rule for the computation of the posteriori probability distribution for model parameters (Tarantola, 2005). If the prior uncertainty in model parameters can be modeled adequately as multivariate Gaussian with mean  $m^{pr}$  and covariance  $C_m$ , and if the observation errors are additive and Gaussian, then to compute the most probable vector of model parameters,  $m^{map}$ , one need only solve for the minimizer of

$$J(m) = \|m - m^{pr}\|_{C_m^{-1}}^2 + \|d_{seis}^{obs} - g_{seis}(m)\|_{C_{d,seis}^{-1}}^2 + \|d_{prod}^{obs} - g_{prod}(m)\|_{C_{d,prod}^{-1}}^2 \quad (4)$$

where  $m$  is the vector of model parameters,  $d_{seis}^{obs}$  is the vector of "observed" seismic attributes,  $d_{prod}^{obs}$  is the vector of observed production data,  $C_{d,seis}$  is the covariance of the noise in the observed seismic attribute and  $C_{d,prod}$  is the covariance of the noise in the production data. The forward model  $g_{seis}(m)$  maps model parameters to simulated seismic attribute data (see Section 3.2) and  $g_{prod}(m)$  maps model parameters to simulated production data (Section 3.3). Real applications generally include other types of data with the same need for characterization of measurement errors. If the data are modeled in the simulator (e.g., RFT measurements), then they are usually included in the production data mismatch term. Core data and porosity log data are usually used in model building and the subsequent uncertainty is included in the prior model mismatch term. There is no requirement in usage of Eq. (4) that the variance in the noise is the same for all data of the same type, but estimation of varying level of uncertainty may be difficult.

Although the Bayesian history matching approach is widely accepted, a number of assumptions limit the general applicability of Eq. (4). First is the assumption that the prior distribution for model parameters can be adequately modeled as multivariate Gaussian. Although Gaussian parameters can often be accomplished through transformation of variables (Bennion and Griffiths, 1966; Freeze, 1975) or through the introduction of latent variables (Armstrong et al., 2003), it is not always the case. Second, there is an assumption that noise in the observations are additive and Gaussian, and that the modeling of the data is perfect, neither of which is valid in general.

In many cases, the weightings of various data mismatch terms in the objective function are given by estimates of the inverse of the measurement error covariance matrix (Dong and Oliver, 2005; Emerick, 2016;

Gosselin et al., 2003; Skjervheim et al., 2007), which can in principle be obtained from the manufacturer of the measurement instrument or computed if the “observations” have been processed. This would be the correct weighting if the assumptions of perfect model and additive Gaussian errors were satisfied.

Although Eq. (4) might be described as the standard objective function for seismic history matching, it is sometimes modified for computational convenience or to account for limitations in the model. In particular, the prior probability term is sometimes omitted, especially when the number of model parameters is small (Chassagne and Aranha, 2020; Ketineni et al., 2020; Stephen et al., 2006), in which case strong assumptions on the prior probability have been implicitly applied through the parameterization, or the term may be omitted because of limitations in the history matching software (Gosselin et al., 2003). The measurement error is often modified to include the effects of modeling error (Section 4.2) and in some cases, a bias correction term is added to the objective function to improve predictability with imperfect models (Lu and Chen, 2020; Oliver and Alfonzo, 2018; Stephen et al., 2009). In many applications, it is additionally assumed for simplicity that the noise in the data is independent, although Liu and Rabier (2002) have shown that this assumption exaggerates the information content in some applications. In Section 4.2.1, we review the evidence for correlated observation errors in both production and seismic data.

Chassagne and Aranha (2020) used synthetic, error-free seismic data to compare four different formulations of the objective function, concluding that the traditional least squares metric gave enough information to perform a good history matching. By neglecting errors in the data, however, they appear to have ignored the most important reason for choosing a measure of the data mismatch. We note that a least squares mismatch is the appropriate form for additive Gaussian error.

Computation of the most probable model parameter values by searching for the minimizer of Eq. (4) requires specification of the observation error covariance matrix  $C_d$  for each data type and specification of the prior model covariance matrix  $C_m$ . It is fairly standard practice to ignore the uncertainty in  $C_d$  and  $C_m$  when history matching, unless the history match was not successful in which case  $C_d$  and  $C_m$  might be modified and the history match repeated. An alternative approach is to use a multiobjective approach for dealing with the conflicting information from the various types of data (Park et al., 2015; Volkov et al., 2018; Watanabe et al., 2017). Although characterization of the observation error is not as critical in this approach, the level of noise does impact the trade-off between the seismic data and the production data (Volkov et al., 2018).

In some cases, additional weights have been applied to various terms in the objective function to reflect the importance of various types of data for history matching (Gosselin et al., 2003; Roggero et al., 2012). This might be done, for example, in a case where two types of data are in conflict and the model has insufficient degrees of freedom to match both, or when one of the data types is more closely related to a quantity of interest. In that case, one might want to ensure that the most important data are well assimilated (and give the data of lesser importance small or zero weight). This appears to be the rationale for increasing the weight on the production data mismatch term in Lorentzen et al. (2019). Haverl et al. (2005) described a somewhat standard objective function, but neglected the prior term and spatial correlations of seismic data errors. They also applied additional weighting of the seismic data term in order to get the seismic data to more strongly influence the results. Because of the other approximations, such as neglect of spatial correlation of seismic data error, it is not clear if the weighting would have been needed if errors had been properly utilized. The objective function for Huang et al. (1997) included weighting factor that allowed the user to vary the relative weighting on the seismic and production data to achieve some desired objective, without providing a rationale for any particular weighting.

Instead of determining an appropriate measurement error for weighting the likelihood, it has been suggested that the quality of seismic data can be determined by analyzing the data in regions of known properties — typically near injection wells where pressure and saturation may be relatively well known. Stephen and MacBeth (2008) propose an approach of this type for characterizing data as good or bad. Bad data could then be ignored in the history matching or given reduced weighting. Similarly, Emerick (2016) eliminated seismic data in regions of the model for which the match was not good. Ignoring data from regions where the match is poor runs the risk of making the model appear to be better than it actually is. Data should of course be down weighted if the quality of the data in a region is expected to be poor because of poor repeatability due to location of an FPSO (Osdal et al., 2006) or because of shadowing effects from overlying reservoir layers (Stephen and MacBeth, 2008).

Although the data assimilation process is often described in Bayesian terms, in which case the weighting of data mismatch terms should be determined by the likelihood function, it is also fairly common to simply choose a level of observation error that corresponds to an “acceptable” level of matching. Examples of this approach include the assumption by Zhang and Leeuwenburgh (2017) of uncorrelated errors in observations of seismic front location with a standard deviation of 100 ft and Avansi et al. (2016) who define an objective function for production data with weighting  $\gamma$  determined by the user, based on acceptability of the mismatch. The potential difficulty of this approach is that it is impossible to investigate the need for improvement in the model parameterization, as the level of misfit is often chosen to allow for model imperfections.

#### 4.2 Total observation error

Errors in some types of data can be readily estimated from knowledge of the instruments used for measurement, but errors in inverted seismic “data” are generally difficult to quantify as the “data” are the result of a lengthy and complex series of processing and inversion steps (Robinson et al., 1986) and they must be compared to models that are inherently imperfect. In this case, the observed seismic attributes can be modeled as consisting of three components: (1) the “true” attribute, (2) an observation error or systematic bias due to processing, and (3) a component of noise due to non-repeatable variations in positioning or surface conditions, etc. For a given set of conditions, actual (processed or inverted) observations are modeled as (Oliver and Alfonzo, 2018)

$$\underbrace{\mathbf{d}_{\text{obs}}}_{\text{actual obs}} = \underbrace{\mathbf{d}_{\text{true}}}_{\text{true obs}} + \underbrace{\boldsymbol{\delta}_o}_{\text{obs error/bias}} + \underbrace{\mathbf{e}_d}_{\text{noise}}.$$

The random error in the observation is assumed to be additive and Gaussian with mean 0 and covariance  $C_d$ . Similarly, the simulated seismic attributes may be modeled as consisting of two components: the true value of the attribute at the same scale as the observation, and a model error or bias component resulting from deficiencies in the model, which for convenience might be modeled as Gaussian, e.g.  $\mathbf{e}_t \sim N[0, C_t]$ ,

$$\underbrace{\mathbf{g}(\mathbf{m})}_{\text{simulated obs}} = \underbrace{\mathbf{d}_{\text{true}}}_{\text{true obs}} + \underbrace{\mathbf{e}_t}_{\text{model error}}$$

where  $\mathbf{m}$  are parameters of the models. Although modeling the bias as a Gaussian random field is straightforward, it requires use of a covariance with a very long range (Oliver and Alfonzo, 2018). A more common approach is to model the bias using basis functions with uncertain coefficients (Kennedy and O’Hagan, 2001). Even if the “true” parameters are used in the model to simulate observations, the simulated data will not match the observed data exactly. The difference will be due to deficiencies in processing and inversion, deficiencies in the forward model, and noise in the data. The last component is the one that is typically referred to as measurement error, but the other

two components may, in fact, have larger magnitudes and are almost certainly correlated.

The total measurement error (or total observation error) can be separated into three components: (1) a component that is result of the lack of repeatability of the measurement, (2) a component that is a result of errors in the processing or seismic inversion, (3) a component that is a result of deficiencies in the forward model of the seismic attributes. Desroziers and Ivanov (2001) and Desroziers et al. (2005) suggest directly estimating the total observation error through analysis of the residuals after data assimilation. Alfonzo and Oliver (2020) applied a similar approach to estimate total observation error for assimilation of 3D seismic data at the Norne Field. Based on a study with controlled model error, they concluded that the correlation range for the total observation error may be between 600 and 2000 m.

#### 4.2.1 Repeatability error (seismic noise)

In almost every approach to history matching, knowledge of the ‘measurement’ error or repeatability error is important for determining the weighting. Even in those cases where a ‘total observation error’ is used instead of the actual measurement error for the weighting, it is often important to know the actual measurement error in order to understand the deficiency in the model and the information that could be gained through model improvement (Oliver, 2020).

In the geophysical literature, the terms measurement error or observation error are not the most common terms. This is perhaps because seismic data are generally processed before inversion, in which case it is the error in the processed data that may be of importance for inversion, and the error in the inverted attributes that may be important for history matching. In neither case, is the quantity that is treated as data actually directly measured.

The term “measurement error” is usually used to describe the lack of repeatability of a measurement (Bland and Altman, 1996), i.e., if a measurement is repeated several times, the measurement will be different each time because of uncontrollable variations in the environment or the equipment. Although seismic surveys may be acquired several times under similar conditions, the results will be different because of variations in wave noise, or human traffic, or geophone positions. Depending on the source of the nonrepeatability, the noise can have both additive and distortion components (Houck, 2007) due to distortion of the wavelet and artifacts introduced during acquisition and processing.

The term seismic noise may also refer to repeatable parts of the signal that do not fit the conceptual model. Thus, Kumar and Ahmed (2020) identifies four categories of seismic noise: (1) ambient sources, (2) wave propagation related noise, (3) data acquisition related noise, and (4) data processing artifacts and notes that even S-wave reflections may be considered noise when the geophysicist is interested in P-wave primary reflections.

In order to estimate the component of seismic measurement error that is not repeatable, it is necessary to have repeated measurements. For time-lapse seismic, the noise can be estimated from the difference in data between different surveys in domains where the seismic signal is expected to be repeatable. Thus, it is common in 4D seismic to estimate the noise in a time-window above the reservoir, unless it is suspected that there have been production induced changes in the overburden. Common measures of repeatability include the normalized root mean square (nrms) and predictability (Kragh and Christie, 2002). The nrms is the difference of the two traces, within a given time window, divided by the average rms of the inputs. Although nrms is used to quantify repeatability, Kragh and Christie (2002) point out that fluctuations observed in nrms may have little to do with signal repeatability but instead depend strongly on the seismic signal strength.

If it is possible to legitimately assume that the seismic noise is characterized by higher frequency than the seismic signal, then it may be possible to filter the image to at least partially separate the noise from the signal, and hence either to denoise the data or to characterize

the data noise covariance. This has been a fairly common approach in the history matching literature (Aanonsen et al., 2003; Emerick, 2016; Luo and Bhakta, 2017; Zhao et al., 2007). This assumption does not appear to be supported by other methods of estimation (Abreu et al., 2005; Alfonzo and Oliver, 2020; Nivlet et al., 2017). Aanonsen et al. (2003) applied this method to a North Sea oil field where they used a moving average filter on normalized and trend-removed data to estimate a correlation range for observation error of approximately 200 m. Using a similar approach, Emerick (2016) estimated the correlation range for 4D seismic data from the Campos basin as 500 m.

In many cases, the estimation of noise is done in a domain that is not expected to show a production response. Stephen et al. (2006) argued, however, that 4D data in the overburden could not be used to assess the data error in the reservoir because of a difference in the migrations, and because of the treatment of imaging at faults. To calculate the covariance of the measurement error, they instead band-pass filtered both seismic and production datasets to separate the data error and estimated signal.

Factorial co-Kriging has been used to separate noise from signal without making the assumption that the noise is spatially uncorrelated or that it is of a much different frequency than the signal (Abreu et al., 2005; Alfonzo and Oliver, 2020; Coléou et al., 2002). In factorial co-Kriging, two surveys could be separated into three parts: a common part that is presumed to derive from the geology, and two spatially independent residual fields that result from non-repeatable sources. Estimates of the non-repeatable part of the data for both surveys can be obtained from both surveys. Abreu et al. (2005) identified a major component of coherent noise in a Canadian heavy oil field with a correlation range of approximately 500 m. Similarly, Alfonzo and Oliver (2020) used factorial co-Kriging to identify coherent noise above the reservoir in the repeat surveys for the Norne field with correlation range of approximately 300 m. Although spatially correlated observation can be characterized using factorial co-Kriging, it is not clear that the results are reliable as the assumptions of stationarity and linearity are unlikely to be valid.

#### 4.2.2 Deficiencies in processing and inversion

The magnitude and source of the observation errors in 4D seismic “data” depends greatly on the level at which the data are matched (Section 2.1). It can be argued that the most basic usable seismic data are seismic amplitudes in two-way travel times. If the data are history matched at the seismic level, then the observed seismic amplitudes may be used for comparison with synthetic seismic amplitudes. The magnitude of the observation error associated with the actual data at well locations can be estimated by doing well ties and comparing synthetic seismograms (“true observation”) in well position with final processed data that has been depth migrated (White and Simm, 2003). This comparison will include some aspects of the forward modeling error including potential errors in the wavelet, but will not account for potential bias in the synthetic seismic in history matching resulting from errors in the PEM.

When the comparison is made at the elastic level, errors in the wavelet will again affect the comparison, but in this case the errors will affect the inversion so they might be considered as part of the actual observation error, while errors in the PEM will again be a part of the modeling error as they will affect the synthetic seismic impedances. In addition, comparison at the elastic level may require additional non-seismic information to extend the seismic frequency band and ultimately quantify absolute values of the underlying elastic parameters. As modern 3D/4D data are produced through high quality acquisition surveys and optimized processing schemes, the main challenge in seismic history matching is not seismic noise but rather bias and errors linked to the forward modeling/inversion (caused by errors in the PEM, geometrical structure, missing model parameters, etc.) and the physical limitations in seismic resolution.

Observation bias has many sources, which can be attributed to seismic acquisition and processing or to deficiencies in seismic inversion. A combined list might include use of a 1D convolutional model, use of the acoustic-wave equation instead of the anisotropic visco-elastic wave equation, imperfections in data processing, uncertain wavelet estimates, and uncertainty on the low-frequency model (Ball et al., 2018; Madsen and Hansen, 2018; Thore, 2015). Lerner et al. (1983) shows that some clear patterns of coherent noise in stacked sections are not seen in the same data when viewed as unstacked traces arranged by common mid-point CMP, indicating that the processing may be one source of coherent noise. Thore (2015) attributes much of the uncertainty in inverted seismic attributes to uncertainties in metaparameters of the inversion or processing. Fixing these parameters at an incorrect value introduces a bias in the processed or inverted attributes. Roach et al. (2015) show that the effect of every step in the processing is to increase the similarity between subsequent surveys as measured by the nrms. The cost of the decrease in variability is generally an increase in bias, however. For qualitative interpretation, the bias may be relatively unimportant, but for quantitative comparison of model to data, the bias cannot be ignored. The notion that correlated observation errors should be expected in highly processed data has been noted in other fields, particularly numerical weather prediction (Fowler et al., 2018; Stewart et al., 2008).

#### 4.2.3 Forward modeling error

Modeling error and observation bias are closely related and, depending on the attributes used for history matching, could have similar sources. For example, if the comparison between observed data and simulated data is made at the saturation and pressure level, then the PEM has been used for inversion and errors in the PEM would result in bias in the observed data. In a more typical case where the data are compared at the level of time shift or impedance, an error in the PEM would result in an error in the forward modeling (model error). The effect on the analysis is similar in both cases, although fixing the error is more straightforward when the error is in the model and can be reduced through the inclusion of additional uncertain parameters.

Modeling of seismic data, i.e. the mapping from model parameters such as reservoir permeability, locations of facies or rock types, fault transmissibilities, pressure dependence on velocity, to seismic attributes has been discussed in Section 3. Many of the sources of model error in 4D seismic history matching are similar to the sources of model error in history matching of production data. Thus errors due to discretization of the fluid flow equations or due to the replacement of the flow simulator by a simulator with approximate physics will affect the ability to match data in both types of history matching. Stephen (2007) and Stephen et al. (2009) discuss the effect of model error resulting from the use of a streamline simulator on seismic history matching problems and discuss methods of compensating for the error in the reservoir simulation. Based on results from Knight et al. (1998) and Stephen (2007) also pointed out that the coarseness of the discretization affects the validity of Gassmann's equation. Hence, a PEM that might be valid at the core scale will not be valid at the simulation scale. Model error resulting from the PEM can also result from choice of an inappropriate model or from fixing the parameters in the PEM at inappropriate values. Alfonzo and Oliver (2020) showed that errors in the PEM could result in model errors that are correlated and have similar magnitudes to the signal.

One of the most common sources of modeling error in any type of history matching is not directly a result of errors in the forward simulation, but a result of missing parameters in the assessment of uncertainty. If there are insufficient degrees of freedom in the model because parameters cannot be modified, then it will generally be difficult or impossible to use parameters that can match data at the appropriate level. Some types of history matching utilize low levels of parameterization. Examples of this type include the use of "gradzones" (Gosselin et al., 2003), pilot points (Stephen et al., 2009) to reduce the number of parameters, or gradual deformation (Roggero et al., 2012), which uses a linear combination of a small number of model realizations to characterize the solution space.

#### 4.3 Dealing with residual model error in 4D SHM

The evidence from the literature shows that model error and observation bias in seismic attributes are correlated and of magnitude that is often larger than that of the measurement error (Madsen and Hansen, 2018; Stephen, 2007; Thore, 2015), in which case it is necessary to include the effect in the weighting of data — data with large model errors or uncorrected bias must be weighted less heavily than other, more accurate data. A relatively easy approach to including model error is to inflate the observation error covariance matrix (Stephen et al., 2006). Vink et al. (2015) describe an approach for estimating a single inflation factor that accounts for model error and bias. Sun et al. (2017) extend that approach to the case in which different inflation factors are used for different data types. It has also been demonstrated that it might be possible to estimate the effect of model error on the total observation error through analysis of the residuals in the data mismatch after model calibration (Alfonzo and Oliver, 2020; Lu and Chen, 2020; Oliver and Alfonzo, 2018). In this case, the observation error covariance is not diagonal.

### 5 Algorithmic methods for big data/big models

Solving the history matching problem amounts to minimizing an objective function. In a properly defined Bayesian case the objective function might be given as in Eq. (4). The history matching problem might alternatively be solved as an inverse problem (non-Bayesian), in which case the prior term in Eq. (4) might either be replaced with a regularization term or omitted. In the latter case other measures will typically, implicitly or explicitly, be used to for regularization of the problem. A common approach will be to reduce the number of parameters. Regardless of how the objective function is going to be minimized, a parameterization of the problem needs to be performed. We will discuss choices with respect to parameterization in Section 5.1, followed by Section 5.2 on data compression. With respect to solving the minimization problem (Eq. (4)), or analogous equations, for instance leaving out the prior term, we will not classify them as Bayesian/non-Bayesian as some of the algorithms might be used with both interpretations. An overview of methodology for minimization is given in Section 5.3. We briefly discuss uncertainty quantification in Section 5.4 and analysis of the reservoir model by interpreting seismic data in Section 5.5.

#### 5.1 Parameterization

A suitable parameterization of the poorly known properties of the subsurface is key for obtaining a good history match. Ideally there should be sufficient degrees of freedom to allow the data to be matched, and to characterize the underlying variability in the subsurface properties, while still allowing efficient numerical calculations. Some of the parameters, such as, vertical and horizontal permeabilities, porosity, net-to-gross ratios, etc., need to be defined on all the numerical grid-cells of the reservoir simulator. For real-field application, the number of grid-cells can be quite large. In the following, we describe some of the parameterization methods which have been applied for history matching of 4D seismic data.

##### 5.1.1 Pilot point

In this method, introduced by Marsily et al. (1984), a number of cells are marked as pilot points and their values are updated independently during the history match. To populate the full reservoir grid with properties, one interpolates between the pilot points using kriging. This method effectively limits the dimension of the history matching problem to the number of pilot points. The method has been utilized for parameterization of geological properties during history matching on several real field cases with 4D seismic data. In many of these studies, permeability and NTG were represented by pilot points (Kazemi

and Stephen, 2012; Kazemi et al., 2011; Stephen and Kazemi, 2014; Stephen and MacBeth, 2008; Stephen et al., 2009, 2006). Strategies for selecting the number, and position of the pilot points, vary among the studies. In Stephen and MacBeth (2008) it was shown that the quality of the history match depends on the position, and density, of the pilot points. Typically, 9–25 pilot points, per well location, have been utilized to represent the petrophysical values on the grid. However, for Stephen and Kazemi (2014), pilot points representing properties within a geological interval were considered as one parameter. Out of 13 wells, 7 wells represented one interval while 6 wells represented two intervals. Hence, uncertainties in NTG, horizontal permeability, and vertical permeability fields were characterized by 19 parameters.

### 5.1.2 Reservoir grid cells

As mentioned above, the reservoir simulator requires that some parameters are represented in every grid-cell on the numerical-grid. It is possible to represent the parameters directly on the grid, and utilize this representation for history matching 4D seismic data. However, retaining such a large number of parameters requires strong prior assumptions. Several studies have utilized this discretization for history matching field cases with 4D seismic data. This method is especially common for ensemble-based methods, as described in Section 5.3.2.

### 5.1.3 Divide and conquer

For some applications it can be efficient to perform a reparameterization of the poorly known parameters. Typically, a reparameterization is applied to reduce the size of the space of parameters. Several methods are available for history matching, see, e.g. Oliver and Chen (2011). The divide and conquer method was introduced as a technique for separating a large history matching problem into manageable sub-problems which can be treated identically using existing algorithms (Sedighi and Stephen, 2010). Using a proxy model one can analyze the interaction between parameters and the misfit. The volume of the parameter space can be subdivided and searched separately, leading to a much more efficient algorithm. The divide and conquer strategy, in combination with pilot points, has been utilized for history matching 4D seismic data for the Nelson field (Stephen, 2018).

## 5.2 Data compression

Reduction of the amount of data may be necessary for several reasons. Seismic information may be available as processed seismic data (e.g., AVO data), inverted attributes (e.g., acoustic impedance), or even raw seismic traces (see also Section 2). Depending on the resolution of the data, selected seismic attribute or feature, and size of the reservoir, the memory requirements for handling the data may vary from gigabytes, terabytes, and even petabytes. There exist several techniques for further reduction of the amount of data. Luo and Bhakta (2017) introduced a compression method based on image denoising and Discrete Wavelet Transforms. In this approach, wavelet coefficients ( $c$ ) are computed using a 3D transform  $c^{\text{obs}} = \text{DWT}(d^{\text{obs}})$ , that decomposes the data ( $d^{\text{obs}}$ ) into a series of wavelets with different frequencies and subbands. Next, an estimate of the noise standard deviation ( $\sigma$ ) for the wavelet coefficients, and a truncation level ( $\tau$ ), are computed. Wavelet coefficients below the truncation level are assumed to be associated with noise, and are removed from the signal using hard thresholding. A compressed signal,  $\hat{c}^{\text{obs}} > \tau$  is then obtained where coefficients with indices denoted  $I$  are kept. During data assimilation the simulated data  $d = g(m)$  are transformed using the same decomposition (i.e. same analyzing wavelet and level of decomposition) as for the actual observations and then compressed as  $\hat{c} = c(I)$ . In the case of correlated noise in the original signal, it is assumed that the noise is transformed to all subbands in the decomposition. The noise for the remaining (kept) wavelet coefficients is represented by a diagonal covariance matrix with the values of  $\sigma^2$  on the diagonal. We note here that all wavelet coefficients are assumed to contain noise, not only the values that are

truncated. Data compression based on DWT is used in a study of the Norne field in Lorentzen et al. (2020). It was also applied and tested on synthetic data in Luo et al. (2017) and Lorentzen et al. (2019).

A different approach is pursued in Soares et al. (2020). Here dictionary learning based on the K-SVD algorithm is used to approximate the data. The dataset is divided into a fixed number of  $N_{fs}$  subsets (patches) and approximated as  $[d_1^{\text{obs}}, \dots, d_{N_{fs}}^{\text{obs}}] \approx D\Gamma$ , where  $D$  is the dictionary matrix and  $\Gamma$  is a sparse matrix computed using an Orthogonal Matching Pursuit (OMP) method. The algorithm is initialized with a Discrete Cosine Transform (DCT) function as the dictionary, and the dictionary is then iteratively updated (learned). The methodology is applied to a synthetic 4D seismic dataset (the Brugge benchmark case) using the RLM-MAC for data assimilation. The authors report that the dictionary learning approach is an efficient method for reducing the amount of data without significant loss of information. A similar approach is pursued in Etienam (2019), but in that paper the PUNQ-S3 reservoir model is investigated using a modified ES-MDA for assimilation.

Finally we mention Liu and Grana (2019) where time-lapse seismic data are compressed to a low-dimensional feature space using a Deep Convolutional Variational Autoencoder (DCAE). The methodology is tested on synthetic datasets, and data assimilation is done using the ES-MDA algorithm. They report improved results using time-lapse seismic and production data compared to production data only, and conclude that the low-dimensional seismic information is valuable for recovering the reservoir properties.

## 5.3 Minimization

In this section we review methodologies for solving the minimization problem (Eq. (4)). We will start by discussing gradient based methods in Section 5.3.1. The ensemble-based methods have become very popular over the last decade and are treated in Section 5.3.2. Then we treat the gradient free methods in Section 5.3.3. Some authors define the history matching problem as a multi-objective minimization problem. We discuss these approaches according to the algorithms used to solve the minimization problem.

### 5.3.1 Gradient methods

A crucial step in utilizing gradient based methods is getting access to the gradients. This can be done in several different ways. The most straight forward might be the *finite-difference method*, where one additional simulation is required for each model variable that is tuned. Due to the significant computation time that is typical with field models, this gives a limitation in the number of variables that can be tuned. More efficient methods are available, as the *forward method* and the *adjoint method*. However, these methods depend on the availability of the products in the simulator, or access to the simulator code. The finite-difference method, forward method and the adjoint method are all described and reviewed in Oliver and Chen (2011). This paper also discusses *streamline-based sensitivities*, which is a fourth approach for approximating sensitivities.

In contrast to the extensive development of gradient-based algorithms for production history matching, there are far fewer examples of the use of gradient-based algorithms for minimizing the objective function for 4D seismic history matching. This might be due both to shifted focus over the last decade towards ensemble-based approaches, but also that obtaining good fit to the 4D seismic data might require higher spatial resolution and therefore more parameters.

*Finite-difference method* By reducing the number of variables to a manageable size, the finite differences approach might be viable and, combined with the gradual deformation method, this approach would still allow spatial variation of the correction fields. Gradual deformation is an approximate method for gradually deforming continuous geostatistical models to achieve a data match. It was originally introduced by Hu (2000) (see also Roggero and Hu, 1998), and utilized for history

matching in e.g., [Hu et al. \(1999\)](#). The principle of the gradual deformation method is that a linear combination of a set of independent Gaussian random functions is also a Gaussian random function. The simplest form of the algorithm has a pair of Gaussian parameter vectors,  $z_1$  and  $z_2$ , combined

$$z(\zeta) = z_1 \cos(\pi\zeta) + z_2 \sin(\pi\zeta)$$

where  $\zeta$  is a deformation parameter. The procedure for history matching using gradual deformation is iterative. First the initial vectors  $z_1$  and  $z_2$  are generated, and the value  $\zeta$  is found by minimizing an objective function. The optimal value  $\zeta^*$  is then used to define a new  $z_1 = z(\zeta^*)$ . By iteratively generating a new  $z_2$  and repeating the minimization procedure, it may be possible to obtain a model that matches data.

The gradual deformation method has been utilized to adjust the petrophysical properties while history matching 4D seismic data in several field cases. [Le Ravalec et al. \(2012\)](#) used gradual deformation to vary the spatial distribution of rock facies and [Roggero et al. \(2007\)](#) used gradual deformation parameters to control the facies realizations in each reservoir unit. Because the final solution must lie in the subspace spanned by the initial vectors,  $z_i$ , it can be difficult to assimilate large amounts of information efficiently ([Liu and Oliver, 2004](#)).

Both in [Le Ravalec et al. \(2012\)](#) and [Roggero et al. \(2007\)](#) (see also [Roggero et al., 2012](#)) history matching was done by optimizing a weighted least square formulation, with terms including both production and seismic data. Both papers utilize the gradual deformation method to simultaneously work with a restricted number of parameters, while still striving to maintain geological realism. In [Roggero et al. \(2007\)](#) an additional element is included for updating facies proportions. [Roggero et al. \(2007, 2012\)](#) reported that gradual deformation with the Powell's dogleg algorithm ([Powell, 1968](#)) was suitable to history match the production data. However, this approach did not work well when 4D seismic data was included. For combined minimization of 4D seismic and production data they proposed a new optimization algorithm based on global adaptive learning of the objective function (response surface fitting of the objective function).

**Forward method** The forward method was implemented in a commercial reservoir simulator, and was exploited for time-lapse history matching in which the number of parameters first were reduced using gradzone analysis ([Bissell, 1994](#)), and a Levenberg–Marquardt approach was utilized for solving the nonlinear least squares system. The methodology was demonstrated on a North Sea field, and a field from the Adriatic sea ([Gosselin et al., 2003](#)). They found that the parameterization using gradzone analysis worked well on a synthetic field example, but was less successful on a real field case. This history matching feature of the commercial reservoir simulator was used by [de Brito et al. \(2010\)](#) for history matching of the Marlim field, a large offshore field in Brazil. The parameters that can be updated using this approach are either regional parameters applied to specific grid blocks or non-regional such as fault transmissibilities and aquifer properties. A limitation of such an approach is related to the selection of parameters and the additional cost of getting the sensitivity for each parameter. [Emerick et al. \(2007\)](#) stated that the additional cost in the gradient calculation is 20% of the cost of one reservoir simulation per parameter, obviously putting a limitation on the number of parameters that can be included in the objective function.

**Adjoint method** For the adjoint method the gradient of the objective function can be obtained with an additional cost of the order of one reservoir simulation ([Emerick et al., 2007](#); [Oliver and Chen, 2011](#)). The adjoint method has been used to compute gradients of the objective function in a number of synthetic 4D seismic history matching studies ([Dong and Oliver, 2005](#); [Emerick et al., 2007](#); [van Essen et al., 2012](#); [Eyidinov et al., 2008](#); [Kahrobaei et al., 2013](#); [Volkov et al., 2018](#)).

The limited-memory Broyden–Fletcher–Goldfarb–Shanno (LBFGS) method, which is a Gauss–Newton type of algorithm, has been utilized

together with gradients obtained utilizing adjoints in a synthetic study motivated from an actual reservoir model to estimate permeability and porosity based on production data and changes in impedances ([Dong and Oliver, 2005](#)). The authors concluded that the data did not provide enough information to get a high resolution characterization of the permeability and porosity, but that improved predictions could be obtained. The LBFGS method has the advantage that it utilize an approximation of the Hessian based on a set of gradients, and is suitable for minimization in large-scale problems. While [Dong and Oliver \(2005\)](#) were able to use the adjoint formulation for 4D seismic data because they had access to the simulator code, [van Essen et al. \(2012\)](#) described a method for using the adjoint feature in a commercial simulator to assimilate saturation data by converting seismic data to pseudo well data. [Kahrobaei et al. \(2013\)](#) presented a workflow for updating structural parameters of the model, specifically the bottom horizon. For the model updating they use a simple descent method. In a synthetic study they found that adding time-lapse seismic data to the production data gave higher spatial resolution and better predictive performance. [Volkov et al. \(2018\)](#) used an adjoint-gradient-based approach for solving a bi-objective history matching problem. The two objectives consisted of the production data and time-lapse seismic data mismatches, respectively. They reported a successful demonstration using synthetic data from a complex 3D model based on the Norne field, and concluded that it will be important to test the methods they have developed on real field cases. The latter statement of course applies to utilizing adjoint methods for 4D seismic history matching in general.

Despite the fact that several groups have investigated the use of adjoints for history matching 4D seismic data, there is a lack of application on real field data. An exception is the work of [Ahmadinia and Shariatipour \(2020\)](#), but in that work only the time-lapse seismic data was used for history matching, focusing on the CO<sub>2</sub> injection at the Sleipner field. This is in contrast to what is observed in another large-scale related inversion problem, seismic full-waveform-inversion (FWI). For seismic FWI of acoustic waves, the adjoint equations are nearly identical to the forward equations and utilizing adjoints is common, also for real world problems. On the other hand, less focus has been paid to quantification of the uncertainty of the solution in the FWI problem ([Virieux et al., 2017](#)).

Some more recent lines of research on utilizing adjoints are presented in [Li et al. \(2020\)](#), [de Moraes et al. \(2020\)](#) and [de Moraes et al. \(2018\)](#). These papers are investigating different new workflows exploiting gradients for coupled processes, as could contain both reservoir flow, rock physics modeling and seismic modeling, which in a longer term can lead to improved workflows for 4D seismic history matching.

**Streamline-based sensitivities** A fourth approach to computing gradients is to utilize streamline based sensitivities. [Watanabe et al. \(2017\)](#) present a streamline-based semi-analytic approach for computing model-parameter sensitivities, accounting for both pressure and saturation effects. They point out that the streamlines can be computed not only from streamline based simulators, but also by post-processing the output from finite-difference simulators. They demonstrated the use of their methodology to update permeability fields on the Norne field, using the provided model for the other parameters.

Although the ensemble-based approach does not utilize gradients, similarities between the ensemble Kalman filter and a Gauss–Newton approach to history matching have been pointed out ([Reynolds et al., 2006](#)). We discuss this similarity in Section 5.3.2.

### 5.3.2 Ensemble methods

In this section we give an overview of the most common ensemble methods used for assimilating seismic data. Currently the industry standard is use of iterative ensemble smoothers that assimilate all available data for each iteration. The benefit compared to traditional Ensemble Kalman Filters (EnKF) is that time consuming restarts of the flow simulator are avoided. For detailed reviews of the traditional

ensemble Kalman filter in reservoir engineering we refer to [Aanonsen et al. \(2009\)](#) and [Oliver and Chen \(2011\)](#).

Consider the objective function (Eq. (4)) introduced in Section 4. The ensemble formulation for this problem is written

$$J(m_j) = \|m_j - m_j^{\text{pr}}\|_{C_m^{-1}}^2 + \|d_j^{\text{obs}} - g(m_j)\|_{C_d}^2, \quad j = 1, \dots, N, \quad (5)$$

where we have simplified the expression by merging  $d^{\text{obs}} = [d_{\text{prod}}^{\text{obs}}, d_{\text{seis}}^{\text{obs}}]$ , and similarly for  $g$  and  $C_d$ . In the above equation each  $m_j^{\text{pr}}$  represents an ensemble member from the (possibly non-Gaussian) prior distribution and  $d_j^{\text{obs}} = d^{\text{obs}} + \epsilon_j$  are perturbed observations using samples  $\epsilon_j$  from the data error distribution  $\mathcal{N}(0, C_d)$ . An updated ensemble ( $m_j$ ) of model realizations are computed by minimizing the objective function for each ensemble member, although it is known that, for a general non-linear observation operator the distribution of samples obtained by minimization is only an approximation of the posteriori distribution. A common feature when deriving the ensemble smoothers is use of the first order Taylor approximation

$$g(m_j^i) \approx g(\bar{m}^i) + g'(\bar{m}^i)(m_j^i - \bar{m}^i), \quad \bar{m}^i = N^{-1} \sum_1^N m_j^i. \quad (6)$$

An exception from this approach is a recently developed ensemble subspace formulation ([Raanes et al., 2019](#); [Evensen et al., 2019](#)) of the Ensemble Randomized Maximum Likelihood method (EnRML) ([Chen and Oliver, 2012](#)). In the subspace formulation approximations are justified using linear regression.

*The Ensemble Smoother with Multiple Data Assimilation (ES-MDA)* ES-MDA was introduced in [Emerick and Reynolds \(2013a\)](#) as an approach to improve the traditional Ensemble Smoother (ES) ([Skjervheim et al., 2011](#)) when working with non-linear problems. Instead of performing a single update step, the algorithm assimilates the data  $N_{\text{MDA}}$  times with inflated noise variance. In the linear Gaussian case, it is shown ([Emerick and Reynolds, 2013a](#)) that multiple data assimilation is equivalent to the single ES data assimilation step. The algorithm is based on the fact that the likelihood term in Bayes formula can, in the Gaussian case, be rewritten as a product of  $N_{\text{MDA}}$  exponential terms with inflated data covariance. The resulting update formula for each ensemble member ( $j = 1, \dots, N$ ) is then given by:

$$m_j^{i+1} = m_j^i + S_m^i (S_d^i)^T (\alpha^i C_d + S_d^i (S_d^i)^T)^{-1} (d^{\text{obs}} + \sqrt{\alpha^i} \epsilon_j - g(m_j^i)), \quad (7)$$

where  $i = 0, \dots, N_{\text{MDA}} - 1$ , and  $\sum_0^{N_{\text{MDA}}-1} \alpha^i = 1$ . In the above equation we use the definitions:

$$S_m^i = (N - 1)^{-\frac{1}{2}} [m_1^i - \bar{m}^i, \dots, m_N^i - \bar{m}^i], \quad (8)$$

$$S_d^i = (N - 1)^{-\frac{1}{2}} [g(m_1^i) - \bar{g}^i, \dots, g(m_N^i) - \bar{g}^i], \quad (9)$$

and  $\bar{g}^i = N^{-1} \sum_1^N g(m_j^i)$ . In order to derive Eq. (7) we set the derivative  $\partial J(m_j)/\partial m_j = 0$  and make use of the approximation  $\tilde{C}_{md}^i \approx g'(\bar{m}^i) \tilde{C}_{mm}^i$ , where  $\tilde{C}_{md}^i = S_m^i (S_d^i)^T$  and  $\tilde{C}_{mm}^i = S_m^i (S_m^i)^T$ . This gradient approximation is justified using the Taylor expansion (Eq. (6)), see e.g. [Chen and Oliver \(2012\)](#).

The ES-MDA method was utilized for 4D seismic history matching of a heavy-oil turbidite reservoir in Campos Basin ([Emerick and Reynolds, 2013b](#)) where results were compared to the results obtained using the standard EnKF. The performance of the methodology was further analyzed in [Emerick \(2016\)](#), where the same field was investigated, but ES-MDA was compared to the standard ES. The conclusions from the papers are that ES-MDA outperformed both the EnKF and the ES in the joint assimilation of production and seismic data, but that the reduction in the ensemble variance was excessive. There exist numerous other applications of ES-MDA for 4D seismic history matching (e.g., [Leeuwenburgh et al., 2016](#); [da Nobrega et al., 2018](#); [Yin et al., 2019](#)). In general, the mismatches to both seismic and production data were reduced at reasonable computational expense.

*The Ensemble Randomized Maximum Likelihood method (EnRML)* EnRML ([Chen and Oliver, 2012](#)) searches for the minimum of the objective functions (Eq. (5)) using an ensemble-based approximation of the Gauss–Newton method. It does not rely on a predefined number of assimilation steps, and differs in that sense from the ES-MDA. The method does, however, require a convergence criteria and the step length parameter is determined by standard line search. The methodology was later improved using the Levenberg–Marquardt algorithm (LM-EnRML), for better selection of the step size and faster convergence ([Chen and Oliver, 2013](#)). However, the original LM-EnRML involves the inverse of the state covariance matrix ( $\tilde{C}_{mm}^i$ ), which is found to be sensitive to the level of truncation in the singular value decomposition (see also the discussion below), which has lead to the most widely used form of the LM-EnRML ignoring the updates from the model mismatch term ( $\tilde{C}_{mm}^i$ ) $^{-1}(m_j^i - m_j^{\text{pr}})$  (see [Chen and Oliver, 2013](#) for details):

$$m_j^{i+1} = m_j^i + S_m^i (S_d^i)^T [(1 + \lambda^i) C_d + S_d^i (S_d^i)^T]^{-1} (d_j^{\text{obs}} - g(m_j^i)), \quad (10)$$

Here  $S_m$  and  $S_d$  are the same as for ES-MDA and given by Eqs. (8) and (9). The Levenberg–Marquardt tuning parameter is denoted  $\lambda^i$ . For details regarding adaptive updates of  $\lambda^i$  we refer to [Chen and Oliver \(2013\)](#).

A flavor of the EnRML is presented in [Luo et al. \(2015\)](#). In that work a Regularized Levenberg–Marquardt algorithm is used to solve a Minimum Average Cost problem (RLM-MAC). The regularization is in this context the model mismatch term, but contrary to the standard EnRML described above, the prior term ( $m_j^{\text{pr}}$  in (5)) is approximated with  $m_j^i$ , thereby circumventing the problematic term ( $\tilde{C}_{mm}^i$ ) $^{-1}(m_j^i - m_j^{\text{pr}})$ . Furthermore, the Taylor expansion (Eq. (6)) is substituted in the objective function before computing the derivative  $\partial J(m_j)/\partial m_j = 0$ , thereby also avoiding the approximation  $\tilde{C}_{md}^i \approx g'(\bar{m}^i) \tilde{C}_{mm}^i$ . The two methods are compared in [Luo et al. \(2015\)](#) and reports better performance for the RLM-MAC algorithm, but as the authors clearly states, the conclusion may be different if the methodologies are investigated on a broader set of experiments. The RLM-MAC was used for sequential assimilation of first production data and then seismic data in a digital twin experiment based on the Norne field ([Lorentzen et al., 2019](#)). That study showed that it was possible to obtain good data match for both data types. In a subsequent study using real data from the Norne field, [Lorentzen et al. \(2020\)](#) showed that it is also possible to assimilate both data types simultaneously, with reduction in mismatch for both production and seismic data.

*Singular value decomposition* All smoothers mentioned above require the inversion of a term like  $[C_d + S_d S_d^T]$  (the step size parameter  $\alpha$  or  $1 - \lambda$ , and iteration index  $i$ , are omitted for simplicity). The term  $S_d$  has size  $N_d \times N$ , and if  $C_d$  is not diagonal or sparse it must be stored as an  $N_d \times N_d$  matrix (the noise associated with seismic data is usually correlated). If the number of observations is large, inverting this matrix can be a time consuming task, even if data compression (Section 5.2) is applied. In addition, the matrix to be inverted is often singular or badly conditioned, especially when the number of measurements is large and many of the data are redundant. Truncated Singular Value Decomposition (TSVD) is a common way of dealing with these issues. In order to avoid working with a dense  $C_d$  we use a sample approximation:

$$C_d \approx S_e S_e^T, \quad \text{where } S_e = (N - 1)^{-\frac{1}{2}} [\epsilon_1 - \bar{\epsilon}, \dots, \epsilon_N - \bar{\epsilon}], \quad \bar{\epsilon} = N^{-1} \sum_1^N \epsilon_j. \quad (11)$$

If the data are of different magnitude it is necessary to scale the observations before performing the TSVD. This can be done by introducing a scaling term, typically selected as a diagonal matrix  $C_{sc}^{1/2}$  where the entries on the diagonal of  $C_{sc}$  are the data error variances. This matrix can be embedded in  $S_e$  and  $S_d$  and in the following we assume this has been done and proceed with the current notation. The TSVD of  $S_d$  is written

$$S_d \approx U_p W_p V_p^T,$$

where  $p \leq N$  is the number of retained singular values. The matrix  $U_p$  is the first  $p$  left-singular vectors with dimension  $N_d \times p$ ,  $W_p$  is a diagonal matrix with the  $p$  largest singular values on the diagonal, and  $V_p$  is a matrix with the  $p$  first right-singular vectors with dimension  $N \times p$ . Following the calculations in Evensen et al. (2019, Sec. 3.4), the inversion is computed

$$(S_e S_e^T + S_d S_d^T)^{-1} \approx (U_p W_p^{-1} Z)(I_N + \Lambda)^{-1} (U_p W_p^{-1} Z)^T,$$

where  $Z$  and  $\Lambda$  is defined through the eigenvalue decomposition

$$W_p^{-1} U_p^T S_e S_e^T U_p W_p^{-1} = Z \Lambda Z^T.$$

Finally we note that after the TSVD we are left with the product  $U_p^T (d_j^{obs} - g(m_j))$ . This projection maps the data onto the row-space of  $U_p^T$  and the data are reduced to a  $p$  dimensional vector.

**Localization** Localization was introduced for ensemble based data assimilation of meteorological and oceanographic models, as a technique to reduce the effect of spurious correlations in estimated covariance matrices, and to increase the number of degrees of freedom in the ensemble. Using a limited ensemble size, sample covariance estimates are bound to significant errors, which results in erroneous updates of parameters. Spurious correlations are typically larger than the true correlations for parameters which are far from the observation location. In addition, it is shown that limited ensemble size combined with large number of measurements leads to underestimation of model uncertainty (Furrer and Bengtsson, 2007). Using localization, the amount of data used to update any specific parameter is reduced, thereby reducing the likelihood of ensemble collapse.

Local analysis (Evensen, 2003; Houtekamer and Mitchell, 1998) (see Fig. 4, left) is a localization technique based on splitting the parameter space into a finite number of patches (a patch could consist of a single gridblock). Each patch is then updated individually, based on measurements located inside the patch, or in a given vicinity of the patch. A benefit of this approach is that the update step can easily be parallelized. However, application to non-local observations is not always straightforward.

Distance based localization (Hamill et al., 2001; Houtekamer and Mitchell, 2001) is a different approach where the full set of parameters is updated simultaneously, but the influence of the available measurements are restricted to certain regions. This is illustrated on the middle plot on Fig. 4. In this case a data point shown as a red dot is used to update parameters that fall inside the green region. The localization domain is usually specified as ellipsoids with given principal semi-axes ( $l$ ) and rotation angles, but any shape is possible. A compact correlation function (e.g., Gaspari and Cohn) is then used to construct a tapering matrix,  $T$ , that has value 1 at the measurement location and gradually decreases to zero at the border of the localization domain. Distance-based localization is often described as a method of covariance regularization, i.e.,  $T \circ \tilde{C}_{mm}$  where  $\circ$  denotes the Schur product. However, the model covariance matrix is not explicitly formed when using ensemble smoothers as described above. As an alternative, the Kalman gain term in Eqs. (7) or (10) is multiplied from the left with the tapering matrix (Chen and Oliver, 2017).

Although distance based localization is efficient in many cases, it can be cumbersome to specify localization domains for large and complex fields with many wells. In addition, the approach cannot be

used for parameters or measurements that do not have a well defined position in space. Parameters used for end-point scaling of relative permeability curves is one example. Correlation based localization (Luo et al., 2018b) was introduced to mitigate the above mentioned problems. This approach involves computation of the correlations ( $r$ ) between the model variables and the simulated observations (or projected observations in case TSVD is used). Further, a threshold value ( $\delta$ ) is computed and a localization domain is defined as the area where  $|r| > \delta$  (Fig. 4, right). The threshold value can be estimated using wavelet-based denoising approach (Luo et al., 2018b), but manual scaling of the estimate may be required. The correlation based localization is adaptive, and both  $r$  and  $\delta$  are updated for each smoother iteration. Correlation based localization has been used to reduce the effects of small ensemble size in history matching of production and seismic data from the Norne Field (Lorentzen et al., 2020).

### 5.3.3 Gradient free methods

**Stochastic neighborhood algorithm** The stochastic neighborhood algorithm was introduced as a method to find a set of models with a good data match in general geophysical inversion problems (Sambridge, 1999). The main idea behind the method is to let the search for new models be guided by all previous forward-model evaluations. Given a set of samples of the parameter, for which the objective function has been evaluated, a Voronoi diagram is generated. That is, a division of the model space into unique cells centered at each sample. Each cell is the nearest neighbor region about the sample with distance measured by the L2 norm. If the objective function is known for all samples, one can make an approximation to the objective function surface by setting the objective function value to a constant inside each Voronoi cell. Evaluating the approximate objective function at any new point in parameter space is then a matter of finding which of the previous samples it is closest to. This proxy surface can be utilized for evaluating the objective function for many different sampling methods. The stochastic neighborhood algorithm has been applied to the problem of history matching of 4D seismic data (e.g. Kazemi and Stephen, 2012; Stephen et al., 2006). In a numerical comparison study, however, Jin et al. (2012a) concluded that the neighborhood algorithm was the least useful of the three methods considered for joint history matching of production and time-lapse-seismic data.

**Monte-Carlo search** Markov Chain Monte-Carlo (MCMC) algorithms are often used to sample from the posterior distribution in Bayesian approaches to inverse problems. One advantage of MCMC methods over minimization-based approaches is that they have some theoretical guarantees of correct sampling even for posterior distributions that are far from Gaussian. In general, however, the conditions that are required to ensure that the sampling is correct, cannot be met in realistic geoscience inverse problems. One particular flavor of MCMC, the *Metropolis-Hastings* algorithm (see Oliver et al., 2008 or Tarantola, 2005 for a short introduction) was suggested for sampling in 4D seismic history matching problems (Huang et al., 1997). The method converged slowly, however, and an ad-hoc modification was made to the acceptance criterion, resulting in a greedy search, which reduced the data misfit more quickly, but lacked clear sampling properties. The greedy approach was also used for a field study in Waggoner et al. (2003). A major problem with this approach is that despite the modification, many iterations are required and the computational cost is high.

An approach based on *discrete Latin hypercube (DLHC) sampling* was developed in a set of synthetic studies (see Maschio and Schiozer, 2016 for details) and later applied to seismic history matching of the Norne G-segment data set (Davolio and Schiozer, 2018). In the latter work the seismic data was included as binary images, and the benchmark case consisting of the G-segment of Norne was used for testing of the methodology. The joint history matching of production and seismic data used 3000 simulations to produce 99 models of the desired quality.

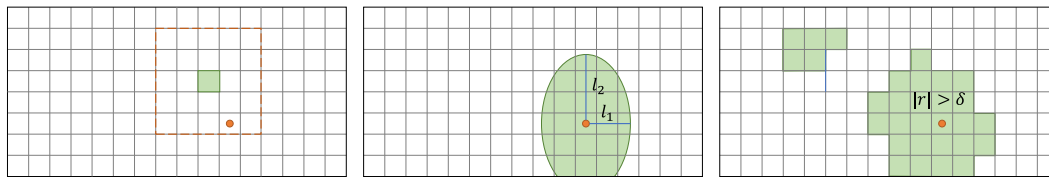


**Fig. 4.** Principles of local analysis (left), distance based localization (middle) and correlation based localization (right). A data point is shown as the red dot. For local analysis, parameters for a given patch (shown in green) are updated based on observations that fall inside a given region around the patch (shown as the red dotted square). Distance based localization is illustrated using an ellipse (with given semi-axes) centered on the observation, and parameters within this ellipse are updated using the observation. The domain obtained using correlation based localization may take any shape, and is not necessarily connected. The domain is determined as the area where the correlations between the observation and the parameters are above a given threshold.

*Simulated annealing* (see Tarantola, 2005 for a short introduction) can be viewed as a variant of the Metropolis–Hastings algorithm designed for minimization, rather than sampling from the posterior probability distribution. In simulated annealing a parameter is introduced, called the ambient temperature by analogy to the physical process of annealing, that is decreased slowly towards zero. This parameter is used in defining Metropolis–Hastings steps, and the construction is such that when the temperature goes towards zero, the successful steps will be closer and closer to the maximum likelihood value. The problem with this approach is that it requires many steps to converge, and it is therefore very time consuming when the objective function is expensive to compute. Ingber (1989) proposed a modification called very fast simulated re-annealing (VFSA) that has been used in geoscience applications. In a comparison of VFSA with stochastic neighborhood algorithm and particle swarm optimization for 4D seismic history matching with a relatively small number of parameters, Jin et al. (2012a) concluded that VFSA was not as useful as particle swarm optimization.

*Particle swarm optimization* (PSO) is an optimization method originally developed as a stylized representation of the movement of organisms in a bird flock or fish school. A set of particles (the swarm) is updated based on the best solution the particle has visited previously and the global optimum found so far. All the particles are updated independently at each iteration of the algorithm, making it easily parallelizable.

Jin et al. (2012a) compared PSO to very fast simulated annealing (VFSA) and the stochastic neighborhood algorithm (see the paragraphs above). Based on results from an initial synthetic study they tested PSO and VFSA on data from a real reservoir. Their objective function included both seismic and production data, but not a prior model mismatch term. A total of 18 continuous and discrete parameters were varied in the search for a match to data. The authors concluded that PSO would be preferred in an environment with resources for parallel computing. In contrast, Tolstukhin et al. (2014) reported that convergence of the PSO method for history matching of seismic data at Ekofisk was slow, and an approach relying on proxy models and multi-dimensional kriging was used instead.

*Evolutionary algorithm* An evolutionary algorithm (EA) is a population-based optimization algorithm, inspired by biological evolution processes. Evolution of an ensemble of models occurs after repeated application of reproduction, mutation, recombination, and selection operators. An advantage of evolutionary algorithms is that they do not make any assumptions about the shape of the posterior distribution. The evolutionary algorithm has been applied for minimizing the objective function for 4D seismic history matching (Chassagne et al., 2016; Obidegwu et al., 2017). In both papers the number of parameters used for optimization has been on the order of 30, and have been selected from a slightly larger set by experimental design methods. A Pareto-based evolutionary algorithm, developed for history matching with multiple objectives, has been applied to the Brugge benchmark case (Park et al., 2015). For this particular problem with the Pareto-based multiobjective evolutionary algorithm performed better than the genetic algorithm that is commonly used in production history matching applications.

#### 5.4 Uncertainty quantification

For works in which a gradient-based method was used for 4D seismic history matching, there been little attention paid to the problem of uncertainty quantification, with the exception of Volkov et al. (2018), in which the randomized maximum likelihood (RML) (see e.g., Oliver and Chen, 2011) method was utilized to find several solutions of the history matching problem. In the RML method, one solves the minimization problem several times, with perturbations of the data term and the mean value for the prior term in Eq. (4). Volkov et al. (2018) applied a bi-objective optimization approach, searching for solutions on a Pareto front. It should be noted that gradients do not directly provide information for uncertainty quantification.

The ensemble Kalman-based methods are generally framed as Monte Carlo approximations of the Bayesian data assimilation problem. The initial ensemble is composed of samples from the prior distribution, while the final ensemble is interpreted as giving an approximation of the posterior uncertainty. However, there are some limitations to this interpretation. For instance, it is well-known that the approaches using a common Kalman gain for all the ensemble members (as the methods discussed in Section 5.3.2) cannot represent the uncertainty in bi-modal distributions.

The MCMC approach is frequently described as the ‘gold-standard’ for sampling from the posterior distribution, but the number of simulations needed to obtain a useful set of independent samples from the posterior distribution is generally infeasible for history matching problems. Other gradient-free methods such as the neighborhood method and the evolutionary methods typically provide a set of history matched models as the output, but in general there is not a clear probabilistic interpretation of the set of samples obtained. Moreover, the fact that one must, in general, reduce the number of parameters implies that the prior uncertainty is underestimated.

#### 5.5 Reservoir analysis

There exist many papers that aim at improved understanding of petroleum reservoirs by interpreting seismic data, but do not use methodology from any of the categories above. Such works contribute either to preparation for assisted history matching, or analysis of the reservoir manually or by trial-and-error. In Alfonzo and Oliver (2019) the suitability of the prior model for the Norne G-segment is investigated using the Mahalanobis distance between measured and simulated time-lapse seismic observations, and necessary improvements of the model are suggested. A different approach to model diagnostics for the Norne field is done in Maleki et al. (2018) where production data and seismic impedance are used to identify regions of the model that need improvement. This work was extended in Maleki et al. (2019), by including a manual history matching procedure for the Norne field. Further, the reliability of the seismic data for the Norne field is investigated in Santos et al. (2018), where manual classification of the data quality is investigated. The prior models for the Namorado field in Campos Basin in Brazil is analyzed in Souza et al. (2018) and acceptance thresholds are used to identify model realization that provide acceptable match with production and seismic amplitudes.

Within the context of reservoir analysis, significant efforts also exist for CO<sub>2</sub> storage. The In Salah field in Algeria is investigated in [Shi et al. \(2019\)](#) using InSAR (Interferometric synthetic aperture radar) uplift data and injection well bottom-hole pressure. The model is improved by manually adjusting the fracture transmissibility thereby providing valuable insight into injection-induced seismicity and fracture flow behavior. CO<sub>2</sub> storage is also analyzed in [Hodneland et al. \(2019\)](#), and here Classification and Regression Tree (CART) is used in combination with a random forest classifier to identify model parameters that are most important for history matching the model.

## 5.6 Summary

- Among the gradient-based methods, utilizing the adjoints seem to be the best alternative as its computation time is not increasing with a growth in the number of parameters. However, we have not found more than one paper ([Volkov et al., 2018](#)) that utilize adjoints on real field data. Moreover, it does not seem that utilizing adjoints and updating a single model give an easy way to provide any uncertainty quantification of the obtained results. In [Volkov et al. \(2018\)](#) the uncertainty quantification was dealt with utilizing the randomized maximum likelihood method, which requires solving one minimization problem for each sample from the posterior distribution. Obviously, the fact that the calculating adjoints are requiring access to the simulator code is hampering its use. If one decide to reduce the number of parameters there are a number of gradient-free approaches available, but out literature review does not pin-point any method being particularly effective.
- The two main ensemble based algorithms for 4D seismic history matching (of real petroleum fields) are ES-MDA and LM-EnRML. There are no clear evidence that one is superior to the other, and both approaches require careful selection of input. For ES-MDA the inflation coefficients ( $\alpha_i$ ) must be chosen based on the characteristics (e.g. non-linearity) of the model. Analysis of the method ([Evensen, 2018](#)) indicates that selecting a decreasing set of inflation coefficients is preferable. This approach is also pursued in [Emerick and Reynolds \(2013b\)](#). Alternatively, the modified ES-MDA ([Emerick, 2016](#)) can be used, but also this approach require selection of ad-hoc hyper-parameters. It is not necessary to specify a fixed number of iterations when using LM-EnRML. However, in real applications where  $C_d$  is inaccurately or poorly specified, careful selection of the convergence criteria is required in order to avoid ensemble collapse. The final solution also depends on initial value for the damping parameter  $\lambda_0$ , and how this parameter is updated during iterations.

## 6 Field applications

Many published investigations of 4D seismic history matching have used synthetic data to illustrate developments in some particular aspect of the workflow, such as the ability to assimilate large amounts of data, or to compare information content from production data and seismic data. In real field cases, the data appear to be more difficult to match than in synthetic cases because many of the assumptions that make the analysis for synthetic cases rigorous are not valid. For real field cases where the consistency of the prior model with reality is not assured, the ‘measurement’ error may be difficult to characterize, and the forward simulators almost certainly lack physical processes that are important to the signal. Thus, perhaps the most important lessons that can be learned from published field cases is how the various limitations of methods and models have been dealt with.

### 6.1 Reservoirs with fluid displacement in relatively homogeneous sands

The Harding Field is relatively simple geologically, with a main reservoir of nearly homogeneous, high porosity sand that is up to 60 meters thick. The 4D seismic data at Harding showed strong signal, which was interpreted as being due to the displacement of oil by water or gas. Several assisted history matches of the 4D seismic data have been reported ([Walker and Lane, 2007](#)), but our discussion will focus on the most recent ([Mitchell and Chassigne, 2019](#)), in which the seismic attributes used for history matching were created from minimum and maximum amplitude maps of the 4D differences over the original oil zone. The difference maps were believed to provide a good representation of water and gas sweep of the oil zone because pressure changes were believed to be small and sand properties were believed to be nearly homogeneous. The maps of saturation change and observed amplitude change were converted to binary maps and were compared on a pixel-by-pixel basis. A differential evolutionary algorithm was used to adjust the values of 7 model parameters to minimize the difference between the observed and simulated 4D binary maps. At the end of the minimization, seismic misfit decreased about 10%. Interestingly, although the geology was simple, the reservoir was nearly homogeneous, and the effect of pressure was thought to be negligible, the comparison between data and model was not made on a traditional seismic attribute.

The Norne Field consists primarily of good-quality sandstones with porosities in the range 25 to 32% and permeabilities on the order of 1 Darcy. Although it appears to be reasonable to model the Norne Field as being composed as a single sand facies with varying clay content ([Suman and Mukerji, 2013](#)), it has not been possible to ignore the effect of cementation layers on vertical communication. The reservoir is partially compartmentalized horizontally by faults and vertically by relatively thin cementation layers ([Osdal et al., 2006](#)). The first seismic survey was performed in 1992 with repeat surveys acquired in 2001, 2003, 2004, 2006, 2008, 2010, 2013 and 2017. Production began in 1997 with water injection for pressure support and improved recovery. The field is currently in tail production. Seismic and production data through 2006 were made available to research groups for evaluation of history matching methods ([Rwechungura et al., 2010](#)). In one of the earlier published studies, [Lygren et al. \(2005\)](#) used differences in acoustic impedance to identify displacement of oil by water. This information was then used, along with RFT data, to modify vertical transmissibility across cementation layers. The parameters used for history matching were rectangular zones of vertical transmissibility multipliers, which had been chosen manually based on visual inspection of the mismatch. Values of the multipliers were estimated using a gradient-based minimization. Again, the magnitude of the seismic data term in the objective function decreased approximately 10% while the RFT mismatch decreased about 15% in the study. The released seismic and production data through 2006 have been recently history matched using an iterative ensemble smoother which allows the use of a far greater number of model parameters. [Lorentzen et al. \(2020\)](#) made use of adaptive localization and data reduction techniques based on truncation of wavelet coefficients. Parameters that were treated as uncertain, and thus adjustable, included gridblock values of permeability (horizontal and vertical), net-to-gross ratio and multipliers for vertical permeability in six layers. Other parameters included initial oil/water contact depths in 5 compartments, multipliers for end-point scaling of relative permeability curves for oil and gas, multipliers for fault transmissibilities, and multipliers for transmissibility between fault block regions. Monthly production data from all wells were assimilated. The magnitudes of the standard deviation of observation errors in production data were selected based on visual inspection of the data. Inverted acoustic impedance differences were used as seismic data. The noise level was estimated to be on the order of 10% of the average value of the 4D impedance differences coming from model based inversion. This level of noise is smaller than the value estimated by [Alfonzo and](#)

Oliver (2019) who estimated that the magnitude of the observation error was about 80% of signal strength. Reservoir behavior in more recent years has become increasingly complex with various competing effects including gas out of solution, re-solution of gas, pressure increase and decrease with possible fracturing, and replacement of oil by water (Osdal and Haverl, 2019).

## 6.2 Fields with complex stratigraphy

Although complex stratigraphy could mean many things, we use this term primarily to describe reservoirs in which the rock properties are determined by facies whose locations are not certain except at well locations. Turbidite reservoirs in which the extent of lobes may be uncertain, or in which ‘packages’ of sand and shale predominate, are the archetypal reservoirs types in this category.

The Nelson Field is a stratigraphically complex field with repeated 3D seismic data with several reports of history matching (Gill et al., 2012; Kazemi et al., 2011; Stephen and Kazemi, 2014). Early published history match results were obtained through manual modification of the net-to-gross ratio, which was identified as the most important variable for modifying changes in predicted acoustic impedance (Gill et al., 2012). In more recent history matching studies (Stephen, 2018), the pilot point method was used to control changes in net-to-gross ratio and permeability (horizontal and vertical). The number of pilot points was restricted by placing pilot points at well locations. Changes in reservoir properties between wells were determined by kriging interpolation. Despite the fact that the Nelson field is believed to be turbiditic, facies were not modified directly in history matching. To quantify the difference between the model and the data, the authors compared inverted acoustic impedance to predicted acoustic impedance, after scaling the observed data to modeled data in regions where predictions were good. Non-repeatable errors in acoustic impedance were estimated in regions of the reservoir where no production-related changes were expected to occur. The neighborhood algorithms was used to generate history matched samples. As discussed in Section 5, the method scales relatively poorly with dimension of the parameter space, so a streamline simulator was used to allow a greater number of simulations. The weightings of the data terms in the objective function were then modified to account for modeling error resulting from the use of the streamline simulator.

The Schiehallion Field is another turbidite reservoir on the UK continental shelf. The most comprehensive study of 4D SHM on this field appears in Stephen et al. (2006). To reduce the influence of model error in this case, the authors chose to use relative impedance for data. They then normalized both observed and predicted attributes, scaling each by the spread. Observation error was estimated by applying a band-pass filter to both seismic and production data to separate signal from noise — assuming that the frequency of the noise was higher than the frequency of the signal. This assumption is unlikely to be valid for production data where allocation error is likely to be correlated for long periods. In any event, the spatial correlation of observation error in seismic was ignored. It is possible that the use of the scaled seismic attributes was successful in removing some of the spatially correlated seismic error. As only five parameters were used for history matching, the information content from data was presumably small, or the model was already mostly calibrated before the reported history matching. The authors also noted that the observed dataset contained several nonproduction-related anomalies (signal where it was not expected) and noted that the magnitude of resolution error was larger than the ‘observation error’. A stochastic neighborhood algorithm was used for minimization. A later study of the same field (Sagitov and Stephen, 2012), used particle swarm optimization to adjust a similar number of parameters. Both methods appeared to be useful for characterizing when the number of parameters to be adjusted was exceedingly small.

The Girassol Field, offshore Angola, is a turbiditic reservoir made up of unconsolidated sands, initially below the bubble point pressure.

The 3D base survey was carried out in late 1999. Production began in December 2001 and gas and water injection was initiated in mid 2002. A monitor survey was carried out at the end of 2002. In the history matching study of Roggero et al. (2012), a truncated plurigaussian model with non-stationary thresholds was used to populate the initial models with facies realizations. One year of production and pressure data from 12 wells was included in the objective function, but at the end of the history matching period, water breakthrough had only occurred in 2 wells and gas breakthrough in one. A weighted least-squares formulation was used to define the objective function, similar to Eq. (4), but neglecting the prior model mismatch term. Parameters that were adjusted to match production data included variogram ranges in petrophysical parameters, average petrophysical properties assigned to each facies, aquifer parameters, fault transmissivity multipliers, and well skin factors. Powell’s dogleg algorithm (Powell, 1968) was used to minimize the production data mismatch. Because the number of parameters was relatively small, it was possible to approximate derivatives of synthetic data with respect to the parameters using finite-differences. After history matching production data, a second stage of history matching was performed with both production data and seismic data. In this stage, real and synthetic acoustic impedance differences were compared and the resulting mismatch was minimized from an optimization algorithm by varying the 3D facies proportions. The weight on the seismic data term was increased by a factor of 16 ‘to balance the influence of 4D seismic data compared to production data’ (Roggero et al., 2012). The ‘observed’ and synthetic acoustic impedance were compared at the geological model scale, so that the simulated dynamic variables from the flow simulator had to be downscaled. The resulting mismatch was minimized from an optimization algorithm by varying the 3D facies proportions. The inversion parameters in the joint inversion were the average proportion of sands in regions with good reservoir properties and the average proportion of shale in regions with the highest pseudo-Vclay.

## 6.3 Complex processes

Fields in which the processes cannot be modeled adequately using a slightly compressible black-oil simulator, include fields with steam or CO<sub>2</sub> injection and fields with large geomechanical effects. In these cases, the cost of simulation increases substantially if the processes are modeled during history matching.

Valhall is a large, initially overpressured chalk field with porosity exceeding 50% in places. The field has been on production since 1982 with large pressure decline and corresponding reservoir compaction and a strong 4D seismic signal for the first 20 years. A permanent reservoir monitoring system was installed in 2003 and full-field water flooding began in 2006. The observed change in seismic attributes has also been exceptionally clear during the water flooding period (van Gestel et al., 2011). Because of the difficulty of rigorous modeling of flow and transport in a strongly compacting reservoir, the simulator used for history matching approximated compaction effects by specifying a pore volume multiplier as a function of reservoir pressure. Two seismic attributes were used as data for comparison: Sum of Negative Amplitudes (SNA) on impedance traces and time shift (TS) in a window above the reservoir. Direct comparison between simulated and ‘observed’ attributes was difficult because of the approximations made in simulation, so the seismic objective function was represented by a map-based correlation value (Kjelstadli et al., 2005). Because of the many approximations in modeling, it was determined that the ‘measurement’ errors could not be used for weighting terms in the objective function. Tolerances and corresponding weights were then determined empirically. Monthly production data from seven wells and a small number of pressure (RFT) surveys were included in the objective function. The objective function did not include a regularization or prior term, but uncertainty ranges were specified for each parameter. The objective function was minimized using a genetic algorithm with

60 parameters including porosity multipliers, permeability multipliers, vertical transmissibility multipliers, pore volume compaction trends, aquifer strength, and wellbore skin values. It was concluded that the various data sets, SNA, TS and production data provided independent spatial information (Kjelstadli et al., 2005). It is difficult, however, to evaluate the quality of any of the matches, although several RFT measurements appear to have mismatch after history matching on the order of 400 psi.

The Ekofisk Field is a large fractured chalk reservoir characterized by high porosity and low permeability. Production began in 1971. Substantial subsidence was observed in late 1984 and large-scale water injection began in 1987. The first 3D seismic survey was acquired two years later. Repeat surveys were acquired in 1999, 2003, 2006 and 2008. After installing a permanent seismic monitoring system in 2010, surveys were acquired approximately twice per year. History matching of time-lapse seismic data at the Ekofisk field is complex for a number of reasons, including the compaction behavior and the belief that flow depends primarily on the fracture network. Reported studies have used the time-strain attribute as data in order to capture most information from the compacting reservoir (Tolstukhin et al., 2012, 2014). Only nine parameters were used for history matching: six parameters that represent the morphing combination coefficients between initial three realizations within the Lower Ekofisk and Upper Tor formations, two parameters to perturb the fracture permeability and one parameter for fracture orientation. An objective function that included oil/gas production and RFT pressures, water production and 4D time-strain was used for history matching. The weight factors for the misfit functions were said to have been normalized for each well and 4D seismic data. The fact that matching could be attempted with such a small number of parameters is undoubtedly a result of the continual model improvement that had occurred in previous history matching exercises. A proxy model was used to replace the reservoir simulator and MCMC was used to develop representative models that match data.

The Sleipner Carbon capture and storage project has injected CO<sub>2</sub> into the Utsira Formation since 1996. As no wells penetrate the reservoir where the CO<sub>2</sub> is accumulating, monitoring of the spread of the plume has primarily been accomplished using repeated 3D seismic surveys acquired in 1994, 1999, 2001, 2004, 2006, 2008, 2010, 2013 and 2016. Surveys up to 2010 are publicly available (Chadwick et al., 2019). Most attempts at history matching have compared simulated spread estimated from changes in velocity with the observed spread (Chadwick et al., 2019; Hodneland et al., 2019; Zhu et al., 2015). Because of the complexity of the physics, most studies have focused on an analysis of the influence of a small number of parameters on the match to seismic interpretation. Zhu et al. (2015) attempted to match data by manually varying lateral permeability anisotropy, the concentration of CH<sub>4</sub> in the CO<sub>2</sub> stream, and reservoir temperatures. Ahmadinia and Shariatipour (2020) fixed the reservoir temperature, permeability anisotropy and CH<sub>4</sub> concentration, but allowed the topseal topography to vary. They used adjoints from a simplified model with vertical equilibrium assumption to compute gradients for the optimization. Williams and Chadwick (2017) included temperature effects in the modeling, but investigated only the effect of heterogeneity. Various authors concluded that it was possible to obtain relatively good matches by introducing permeability anisotropy or the introduction of permeability heterogeneity. Others suggested that calibration of temperature was sufficient, and others allowed only the topseal topography to vary. Because the effects of parameters were often studied independently, the extreme limitations in the selection and in the number of parameters allowed to vary makes any conclusions about uncertainty impossible.

There have been a relatively large number of applications of 4D seismic history methods to fields with thermal stimulation. Hetz et al. (2017) describe an application of history matching to a single cycle of a cyclic steam stimulation operation at one pad in the Peace River Field, Alberta, Canada. A seismic monitoring system had been installed in 2014, allowing daily time lapse seismic surveys. Because the reservoir

under study had been previously subjected to many cycles of steam injection and soaking, the initial condition at the start of the current cycle was uncertain. Maps of seismic time shift (relative to the base survey) were computed for each of the 82 monitor surveys measured during the stimulation cycle. Then a single map of 'onset time' was estimated. This was the calendar time at every location at which the change in seismic time shift from the base survey exceeded the threshold value of 0.1 ms. History matching was performed in two stages. In the first stage, low frequency components of the initial saturation field, initial temperature field, porosity field, and the permeability field were adjusted using an evolutionary algorithm. In the second stage, the permeability field for several models from the first stage was adjusted on a cell-by-cell basis using sensitivities estimated using streamline computations.

Although the authors used a rock physics model to compute time shifts for the simulated properties, the computed 'onset time' appeared to be less sensitive to errors in the rock physics model than the time shift themselves, thus the effect of modeling error on history matching was reduced. The use of onset time with an evolutionary algorithm appears to have been successful in obtaining multiple models that matched the onset data and the BHP data during the first half of a stimulation cycle. In this field example, however, the changes in the states (temperature, water saturation and pressure) were monotonic during the history matching period. It is not clear how well the methodology would work for fields for which the timescale for changes in operating conditions is similar to or shorter than the frequency of monitoring surveys.

#### 6.4 Comments on field cases

- Despite the complexity of several of the fields and the large number of published papers on the importance of model realism, the locations of facies boundaries were updated in only one of the seismic history matching field studies (Roggero et al., 2012). Either including uncertainty in facies distributions is not as important as sometimes believed, or it is simply too difficult to do in a meaningful way in realistic field cases. We suspect that there may be some truth to both justifications.
- Although carbonate reservoirs hold much of the world's oil reserves, the application of 4D seismic history matching to carbonate reservoirs, other than chalk reservoirs, is extremely limited. This appears to be partially a result of the stiffness of the matrix which makes detection of saturation changes difficult and partially a result of the complexity of modeling the permeability heterogeneity in carbonate reservoirs.
- Of the nine field applications described in this section, the history matching was performed at the elastic level in five applications and at the seismic level in three. The remaining case is difficult to characterize as the actual observations (time-shift) were at the seismic level, but the observations were thresholded and compared with a saturation map. None of the field examples used inversion of seismic data to the pressure or saturation level.
- Limitations in the model have been dealt with several ways. In some cases, the magnitude of the observation error has been inflated to partially account for the inadequacy of the model. In other cases, the data has been specifically chosen to limit the effect of modeling error. In many cases, the specification of level of observation error was chosen in an ad hoc manner, which might have implicitly accounted for model error.
- Although many of the field cases have been carried out carefully, it is difficult to describe any as truly 'successful'. A really successful SHM would need to match the data to the correct level (which is difficult to characterize), and would need to use an appropriate regularization/prior term that is neither too restrictive or too flexible, and would generate samples from the potentially nongaussian posterior. None of the cases fulfilled all of these requirements.

- In many of the case studies, the number of parameters to be adjusted was reduced to exceptionally small values through sensitivity studies that identified the parameters that were most important for matching observations. The reduced parameterization in these cases appears to largely a necessity resulting from type of optimization algorithms chosen. Any approach that does not allow a large number of parameters is clearly ignoring uncertainty in parameters that may be influential in forecast uncertainty.

## 7 Summary

Despite the desirability of integrating 4D seismic data into reservoir model characterization, it appears that the problem of history matching 4D seismic data is much more difficult than history matching production data. There are a number of contributors to the difficulty, but it does not appear to be primarily a result of limitations in data assimilation algorithms, which are capable of assimilating large numbers of data into models with large numbers of parameters. Although state-of-the-art data assimilation methods for large problems are still not capable of rigorous uncertainty quantification, it appears to us that the biggest challenges are in the modeling of seismic data and the proper weighting of the mismatch between observed and modeled seismic data or attributes. Modeling of pressure sensitivity of seismic attributes has been particularly uncertain as it is typically based on measurement of elastic properties on core samples whose properties might have been altered in the coring and retrieval process. Uncertainty in the pressure dependence has not yet been accounted for in the history matching workflows.

It is difficult to characterize the appropriate weighting of seismic data against production data and prior information, partly because seismic data tends to be highly processed and partly because modeling of seismic attributes is often highly simplified. Nevertheless, when actual data are compared to simulated data, it is clearly not sufficient to use only “measurement error” for weighting; it is necessary to account for modeling error due to missing physics and missing parameters or for bias introduced through processing and inversion of seismic attributes. Seismic data error for 4D seismic history matching will always be correlated and the correlation length may be similar to the correlation length of the signal. It is clear that many of the important issues related to weighting of model error have been recognized for many years (Gosselin et al., 2003), yet implementation of solutions has remained a challenge.

Despite the difficulty of characterizing errors in the seismic attribute data, it is important that the error should at least be estimated. For history matching, Aanonsen et al. (2003) showed that assuming the incorrect value for  $C_D$  limits the usefulness of seismic data in history matching and for synthetic examples, minimization of an objective function with an inappropriate  $C_D$  resulted in a suboptimal solution. Similar conclusions have been made for numerical weather forecasting. A second important reason for attempting to correctly characterize the observation error is that the characteristics of non-repeatable 4D noise should be an important consideration when choosing the optimal domain in which to integrate seismic, borehole and reservoir engineering data. In particular, Souza et al. (2017) showed that noise can be incorrectly interpreted as signal when  $C_D$  is poorly characterized. Finally, even when performing synthetic studies, it is important to use realistic noise models as the conclusions are influenced by the type of noise (Birmie et al., 2020).

In practical applications of seismic history matching with a petroelastic model, the seismic data appear to most commonly be represented as maps of seismic attributes (i.e., computed over a time window) as this has the advantage of robustness with perhaps only small loss of resolution when compared with cubes of attributes. For thick formations, multiple maps have been used when loss of resolution from a single map would be excessive. It also appears that attributes are

most commonly assimilated at either the seismic level (e.g., time-shift or amplitude) or at the elastic level (e.g., acoustic impedance), but seldom at the simulation level. Assimilation at the seismic level has the advantage of avoiding the need for seismic inversion, although the consequence is that forward modeling of the seismic data must be performed repeatedly for comparison of modeled with actual data.

Field cases provided insight into practical approaches to dealing with deficiencies in the model. In some cases, the magnitude of the observation error has been inflated to partially account for the inadequacy of the model and the consequent inability to provide a match at the expected level. In other cases, the type of data has been specifically chosen to reduce the effect of modeling error in the PEM (e.g., fronts or binary fields). In many cases, it appears that the specification of magnitude of observation error was chosen in an ad hoc manner, which might have implicitly accounted for model error.

For inverse problems with large, complex models and large numbers of observations, the history matching methods can generally be divided into two classes: one in which the focus is on the potential nongaussianity of the probability density after history matching and a second in which the focus is on the ability to assimilate large numbers of observations by adjusting large numbers of variables. The first category can perhaps be represented by evolutionary methods or particle swarm methods. Although neither method actually provides a representation of the posterior probability density, they are capable of identifying multiple peaks when the number of parameters is not large. The second category is best represented by ensemble-Kalman smoother type algorithms which have been used for problems with tens of thousands of observations and millions of model parameters. This class of methods uses approximations of the model covariance for updating and is therefore most useful when the posterior probability density is unimodal. We currently believe that the ensemble-Kalman based approach is more appropriate as it allows more degrees of freedom and consequently less loss of information. Developing methods capable of providing a rigorous assessment of uncertainty for large nonlinear data assimilation problems such as 4D seismic history matching is still a challenge.

Although it appears that data assimilation or history matching algorithms are capable of calibrating large models to large data sets, data assimilation is only a part of an entire workflow. It is difficult, for example, to describe any of the field cases as truly ‘successful’ as none of the cases demonstrated systematic and rigorous quality assessment for the history matched models. A really successful SHM would need to match the data to the correct level (which is determined by the total observation error and hence difficult to characterize), and would need to use an appropriate regularization/prior term that is neither too restrictive or too flexible, and would generate samples from the potentially nongaussian posterior. None of the field cases fulfilled all of these requirements. Additionally, a full workflow requires the opportunity to improve models, not simply calibrate parameters. There is currently a lack of automated methods for model improvement. This is clearly also a problem for production history matching, but the need for model improvement may not be as obvious in production history matching because the information content is lower when 4D seismic data are neglected.

Finally, in many of the case studies, the number of parameters to be adjusted was exceedingly small. The reduced parameterization in these cases appears to have been largely a necessity resulting from the type of optimization algorithms chosen. If these history matches were actually successful in the sense that they indeed matched data at the appropriate level, then one would have to conclude either that the amount of information in the 4D seismic data was exceedingly small, or that much of the information in the seismic data was assimilated into the ‘base’ model before the automated or assisted history matching occurred. If the goal of history matching is extremely limited, then perhaps only a small amount of information is important. An approach that relies on small numbers of parameters is unlikely to adequately characterize uncertainty.

## Declaration of competing interest

The authors declare that they have no known competing financial interests or personal relationships that could have appeared to influence the work reported in this paper.

## Acknowledgments

The authors acknowledge financial support from the NORCE research cooperative research project "Assimilating 4D Seismic Data: Big Data Into Big Models" which is funded by industry partners, Equinor Energy AS, Norway, Lundin Energy Norway AS, Repsol Norge AS, Norway, Shell Global Solutions International B.V., Norway, Total E&P Norge AS, Norway, and Wintershall Dea Norge AS, Norway, as well as the Research Council of Norway through the Petromaks2 program (NFR project number: 295002). The authors also acknowledge the Research Council of Norway and the industry partners, ConocoPhillips Skandinavia AS, Norway, Aker BP ASA, Norway, Vår Energi AS, Norway, Equinor Energy AS, Norway, Neptune Energy Norge AS, Lundin Energy Norway AS, Halliburton AS, Norway, Schlumberger Norge AS, Norway, and Wintershall Dea Norge AS, Norway, of The National IOR Centre of Norway for support.

## References

- Aanonsen, S.I., Aavatsmark, I., Barkve, T., Cominelli, A., Gonard, R., Gosselin, O., Kolasinski, M., Reme, H., 2003. Effect of scale dependent data correlations in an integrated history matching loop combining production data and 4D seismic data. In: Proc SPE RSS. The Woodlands. <http://dx.doi.org/10.2118/79665-MS>.
- Aanonsen, S.I., Nævdal, G., Oliver, D.S., Reynolds, A.C., Vallès, B., 2009. The ensemble Kalman filter in reservoir engineering - a review. SPE J. 14, 393–412. <http://dx.doi.org/10.2118/117274-PA>.
- Abreu, C.E., Lucet, N., Nivlet, P., Royer, J.J., 2005. Improving 4D seismic data interpretation using geostatistical filtering. In: 9th International Congress of the Brazilian Geophysical Society. <http://dx.doi.org/10.1190/sbgf2005-248>.
- Ahmadinia, M., Shariati, S.M., 2020. Analysing the role of caprock morphology on history matching of Sleipner CO<sub>2</sub> plume using an optimisation method. Greenh. Gases: Sci. Technol. 10, 1077–1097. <http://dx.doi.org/10.1002/ghg.2027>.
- Alerini, M., Ayzenberg, M., Ek, T., Feng, T., Hustoft, L., Lie, E., Liu, S., Skjei, N., Skjervheim, J.A., 2014. Utilization of time-lapse seismic for reservoir model conditioning. In: 76th EAGE Conference and Exhibition 2014. European Association of Geoscientists & Engineers, pp. 1–5. <http://dx.doi.org/10.3997/2214-4609.20141144>.
- Alfi, M., Hosseini, S.A., 2016. Integration of reservoir simulation, history matching, and 4D seismic for CO<sub>2</sub>-EOR and storage at Cranfield, Mississippi, USA. Fuel 175, 116–128. <http://dx.doi.org/10.1016/j.fuel.2016.02.032>.
- Alfonzo, M., Oliver, D.S., 2019. Evaluating prior predictions of production and seismic data. Comput. Geosci. 23, 1331–1347. <http://dx.doi.org/10.1007/s10596-019-09889-6>.
- Alfonzo, M., Oliver, D.S., 2020. Seismic data assimilation with an imperfect model. Comput. Geosci. 24, 889–905. <http://dx.doi.org/10.1007/s10596-019-09849-0>.
- Alfred, D., Atan, S., Hamman, J.G., Caldwell, D.H., 2008. Petro-elastic models-how many and at what scale?. In: Europec/EAGE Conference and Exhibition. Society of Petroleum Engineers, <http://dx.doi.org/10.2118/113854-MS>.
- Amini, H., 2014. A Pragmatic Approach to Simulator-to-Seismic Modelling for 4D Seismic Interpretation (Ph.D. thesis). Heriot-Watt University.
- Amini, H., MacBeth, C., Shams, A., 2020. Seismic modelling for reservoir studies: a comparison between convolutional and full-waveform methods for a deep-water turbidite sandstone reservoir. Geophys. Prospect. 68, 1540–1553. <http://dx.doi.org/10.1111/1365-2478.12936>.
- Armstrong, M., Galli, A.G., Loc'h, G.L., Geffroy, F., Eschard, R., 2003. Plurigaussian Simulations in Geosciences. Springer, New York.
- Avansi, G.D., Maschio, C., Schiozer, D.J., 2016. Simultaneous history-matching approach by use of reservoir-characterization and reservoir-simulation studies. SPE Reserv. Eval. Eng. 19, 694–712. <http://dx.doi.org/10.2118/179740-PA>.
- Avseth, P., Skjei, N., 2011. Rock physics modeling of static and dynamic reservoir properties—a heuristic approach for cemented sandstone reservoirs. Lead. Edge 30, 90–96. <http://dx.doi.org/10.1190/1.3535437>.
- Avseth, P., Skjei, N., Mavko, G., 2016. Rock-physics modeling of stress sensitivity and 4D time shifts in patchy cemented sandstones—application to the Visund Field, North Sea. Lead. Edge 35, 868–878. <http://dx.doi.org/10.1190/le35100868.1>.
- Avseth, P., van Wijngaarden, A.J., Mavko, G., Johansen, T.A., 2006. Combined porosity, saturation and net-to-gross estimation from rock physics templates. In: SEG Technical Program Expanded Abstracts 2006. Society of Exploration Geophysicists, pp. 1856–1860. <http://dx.doi.org/10.1190/1.2369887>.
- Ayzenberg, M., Hustoft, L., Skjei, N., Feng, T., 2013. Seismic 4D inversion for quantitative use in automated history matching. In: 75th EAGE Conference & Exhibition Incorporating SPE EUROPEC 2013. European Association of Geoscientists & Engineers, <http://dx.doi.org/10.3997/2214-4609.20130457>.
- Aziz, K., Settari, A., 1979. Petroleum Reservoir Simulation. Elsevier Applied Science, New York.
- Ball, V., Tenorio, L., Schiott, C., Blangy, J.P., Thomas, M., 2018. Uncertainty in inverted elastic properties resulting from uncertainty in the low-frequency model. Lead. Edge 34, 1028–1035. <http://dx.doi.org/10.1190/le34091028.1>.
- Batzle, M., Wang, Z., 1992. Seismic properties of pore fluids. Geophysics 57, 1396–1408. <http://dx.doi.org/10.1190/1.1443207>.
- Bennion, D.W., Griffiths, J.C., 1966. A stochastic model for predicting variations in reservoir rock properties. SPE J. 6, 9–16. <http://dx.doi.org/10.2118/1187-PA>.
- Bhakta, T., 2018. Improvement of pressure-saturation changes estimations from time-lapse PP-AVO data by using non-linear optimization method. J. Appl. Geophys. 155, 1–12. <http://dx.doi.org/10.1016/j.jappgeo.2018.04.020>.
- Bhakta, T., Tolstukhin, E., Pacheco, C., Luo, X., Nævdal, G., 2018. Petrophysical parameters inversion from seismic data using an ensemble-based method - A case study from a compacting reservoir. In: ECMOR XVI-16th European Conference on the Mathematics of Oil Recovery. European Association of Geoscientists & Engineers, <http://dx.doi.org/10.3997/2214-4609.201802143>.
- Bhakta, T., Tolstukhin, E., Pacheco, C., Luo, X., Nævdal, G., 2020. Decoupling of changes in pressure-saturation and porosity fields from time-lapse seismic data using an ensemble based method for a compacting chalk reservoir. In: SEG Technical Program Expanded Abstracts 2020. Society of Exploration Geophysicists, pp. 3739–3743. <http://dx.doi.org/10.1190/segam2020-3423752.1>.
- Birnie, C., Chambers, K., Angus, D., Stork, A.L., 2020. On the importance of benchmarking algorithms under realistic noise conditions. Geophys. J. Int. 221, 504–520. <http://dx.doi.org/10.1093/gji/ggaa025>.
- Bissell, R., 1994. Calculating optimal parameters for history matching. In: 4th European Conference on the Mathematics of Oil Recovery. European Association of Geoscientists & Engineers, <http://dx.doi.org/10.3997/2214-4609.201411181>.
- Bland, J.M., Altman, D.G., 1996. Measurement error. Br. Med. J. 313, 744. <http://dx.doi.org/10.1136/bmj.312.7047.1654>.
- Bogan, C., Johnson, D., Litvak, M., Stauber, D., 2003. Building reservoir models based on 4D seismic & well data in Gulf of Mexico oil fields. In: SPE Annual Technical Conference and Exhibition. Society of Petroleum Engineers, <http://dx.doi.org/10.2118/84370-MS>.
- Bosch, M., Mukerji, T., Gonzalez, E., 2010. Seismic inversion for reservoir properties combining statistical rock physics and geostatistics: A review. Geophysics 75, 75A165–75A176.
- Briceño, A., 2017. Calibration and Use of the Petroelastic Model for 4D Seismic Interpretation (Ph.D. thesis). Heriot-Watt University, Edinburgh.
- de Brito, D., de Moraes, R., Emerick, A., 2010. The Marlim field: Incorporating time-lapse seismic in the assisted history matching. In: SPE Latin American & Caribbean Petroleum Engineering Conference. Society of Petroleum Engineers, <http://dx.doi.org/10.2118/137763-MS>.
- Brynjarsdóttir, J., O'Hagan, A., 2014. Learning about physical parameters: the importance of model discrepancy. Inverse Problems 30, 114007. <http://dx.doi.org/10.1088/0266-5611/30/11/114007>.
- Buland, A., Omre, H., 2003. Bayesian linearized AVO inversion. Geophysics 68, 185–198.
- Castro, S.A., Caers, J., Otterlei, C., Meisingset, H., Hoye, T., Gomel, P., Zachariassen, E., 2009. Incorporating 4d seismic data into reservoir models while honoring production and geologic data: A case study. Lead. Edge 28, 1498–1505.
- Chadwick, R., Williams, G., Falcon-Suarez, I., 2019. Forensic mapping of seismic velocity heterogeneity in a CO<sub>2</sub> layer at the Sleipner CO<sub>2</sub> storage operation, North Sea, using time-lapse seismics. Int. J. Greenh. Gas Control 90, 102793. <http://dx.doi.org/10.1016/j.ijggc.2019.102793>.
- Chassagne, R., Aranha, C., 2020. A pragmatic investigation of the objective function for subsurface data assimilation problem. Oper. Res. Perspect. 7, 100143. <http://dx.doi.org/10.1016/j.orp.2020.100143>.
- Chassagne, R., Obidegwu, D., Dambrine, J., MacBeth, C., 2016. Binary 4D seismic history matching, a metric study. Comput. Geosci. 96, 159–172. <http://dx.doi.org/10.1016/j.cageo.2016.08.013>.
- Chen, Z., Huan, G., Ma, Y., 2006. Computational Methods for Multiphase Flows in Porous Media. Computational Science and Engineering, Society for Industrial and Applied Mathematics, Philadelphia, <http://dx.doi.org/10.1137/1.9780898718942>.
- Chen, Y., Oliver, D.S., 2012. Ensemble randomized maximum likelihood method as an iterative ensemble smoother. Math. Geosci. 44, 1–26. <http://dx.doi.org/10.1007/s11004-011-9376-z>.
- Chen, Y., Oliver, D.S., 2013. Levenberg-Marquardt forms of the iterative ensemble smoother for efficient history matching and uncertainty quantification. Comput. Geosci. 17, 689–703. <http://dx.doi.org/10.1007/s10596-013-9351-5>.
- Chen, Y., Oliver, D.S., 2017. Localization and regularization for iterative ensemble smoothers. Comput. Geosci. 21, 13–30. <http://dx.doi.org/10.1007/s10596-016-9599-7>.
- Coléou, T., Hoerber, H., Lecerf, D., et al., 2002. Multivariate geostatistical filtering of time-lapse seismic data for an improved 4D signature. In: 73rd Ann. Intern. Mtg. SEG, Expanded Abstracts. <http://dx.doi.org/10.1190/1.1816995>.

- Côrte, G., Dramsch, J., Amini, H., MacBeth, C., 2020. Deep neural network application for 4D seismic inversion to changes in pressure and saturation: Optimizing the use of synthetic training datasets. *Geophys. Prospect.* 68, 2164–2185. <http://dx.doi.org/10.1111/1365-2478.12982>.
- Dadashpour, M., Landrø, M., Kleppe, J., 2008. Nonlinear inversion for estimating reservoir parameters from time-lapse seismic data. *J. Geophys. Eng.* 5, 54–66. <http://dx.doi.org/10.1088/1742-2132/5/1/006>.
- Danaei, S., Neto, G.M.S., Schiozer, D.J., Davolio, A., 2020. Using petro-elastic proxy model to integrate 4D seismic in ensemble based data assimilation. *J. Pet. Sci. Eng.* <http://dx.doi.org/10.1016/j.petrol.2020.107457>.
- Davolio, A., Schiozer, D.J., 2018. Probabilistic seismic history matching using binary images. *J. Geophys. Eng.* 15, 261–274. <http://dx.doi.org/10.1088/1742-2140/aa99f4>.
- Davolio, A., Schiozer, D., 2019. A proper data comparison for seismic history matching processes. In: SPE Europec Featured At 81st EAGE Conference and Exhibition. <http://dx.doi.org/10.2118/195549-ms>.
- Desroziers, G., Berre, L., Chapnik, B., Poli, P., 2005. Diagnosis of observation, background and analysis-error statistics in observation space. *Q. J. R. Meteorol. Soc.* 131, 3385–3396. <http://dx.doi.org/10.1256/qj.05.108>.
- Desroziers, G., Ivanov, S., 2001. Diagnosis and adaptive tuning of observation-error parameters in a variational assimilation. *Q. J. R. Meteorol. Soc.* 127, 1433–1452. <http://dx.doi.org/10.1002/qj.49712757417>.
- Dong, Y., Oliver, D.S., 2005. Quantitative use of 4D seismic data for reservoir description. *SPE J.* 10, 91–99. <http://dx.doi.org/10.2118/84571-PA>.
- Emami Niri, M., Lumley, D.E., 2015. Simultaneous optimization of multiple objective functions for reservoir modeling. *Geophysics* 80, M53–M67. <http://dx.doi.org/10.1190/GEO2015-0006.1>.
- Emerick, A.A., 2016. Analysis of the performance of ensemble-based assimilation of production and seismic data. *J. Pet. Sci. Eng.* 139, 219–239. <http://dx.doi.org/10.1016/j.petrol.2016.01.029>.
- Emerick, A.A., de Moraes, R.J., Rodrigues, J.R.P., 2007. History matching 4D seismic data with efficient gradient based methods. In: SPE Europec/EAGE Annual Conference and Exhibition. Society of Petroleum Engineers, <http://dx.doi.org/10.2118/107179-MS>.
- Emerick, A.A., Reynolds, A.C., 2012. History matching time-lapse seismic data using the ensemble Kalman filter with multiple data assimilations. *Comput. Geosci.* 16, 639–659. <http://dx.doi.org/10.1007/s10596-012-9275-5>.
- Emerick, A.A., Reynolds, A.C., 2013a. Ensemble smoother with multiple data assimilation. *Comput. Geosci.* 55, 3–15. <http://dx.doi.org/10.1016/j.cageo.2012.03.011>.
- Emerick, A.A., Reynolds, A.C., 2013b. History-matching production and seismic data in a real field case using the ensemble smoother with multiple data assimilation. In: SPE Reservoir Simulation Symposium. The Woodlands, Texas, USA. <http://dx.doi.org/10.2118/163675-MS>.
- Enchery, G., Ravalec-Dupin, L., Roggero, F., 2007. An improved pressure and saturation downscaling process for a better integration of 4D seismic data together with production history. In: EUROPEC/EAGE Conference and Exhibition. Society of Petroleum Engineers, <http://dx.doi.org/10.2118/107088-MS>.
- van Essen, G., Jimenez, E., Przybysz-Jarnut, J., Horesh, L., Douma, S., van den Hoek, P., Conn, A., Mello, U.T., 2012. Adjoint-based history matching of production and time-lapse seismic data. In: EAGE Annual Conference & Exhibition Incorporating SPE Europec. Society of Petroleum Engineers, <http://dx.doi.org/10.2118/154375-MS>.
- Etienam, C., 2019. 4D seismic history matching incorporating unsupervised learning. In: SPE Europec featured at 81st EAGE Conference and Exhibition. London, England, UK. <http://dx.doi.org/10.2118/195500-MS>.
- Evensen, G., 2003. The ensemble Kalman filter: Theoretical formulation and practical implementation. *Ocean Dyn.* 53, 343–367. <http://dx.doi.org/10.1007/s10236-003-0036-9>.
- Evensen, G., 2018. Analysis of iterative ensemble smoothers for solving inverse problems. *Comput. Geosci.* 22, 885–908. <http://dx.doi.org/10.1007/s10596-018-9731-y>.
- Evensen, G., Raanes, P.N., Stordal, A.S., Hove, J., 2019. Efficient implementation of an iterative ensemble smoother for data assimilation and reservoir history matching. *Front. Appl. Math. Stat.* 5, 1–47. <http://dx.doi.org/10.3389/fams.2019.00047>.
- Eydinov, D., Aanonsen, S.I., Haukås, J., Aavatsmark, I., 2008. A method for automatic history matching of a compositional reservoir simulator with multipoint flux approximation. *Comput. Geosci.* 12, 209–225. <http://dx.doi.org/10.1007/s10596-007-9079-1>.
- Fagervik, K., Lygren, M., Valen, T.S., Hetlelid, A., Berge, G., Dahl, G.V., Sønneland, L., Lie, H.E., Magnus, I., 2001. A method for performing history matching of reservoir flow models using 4D seismic. In: SEG Technical Program Expanded Abstracts 2001. Society of Exploration Geophysicists, pp. 1636–1639. <http://dx.doi.org/10.1190/1.1816429>.
- Fahimuddin, A., Aanonsen, S.I., Skjervheim, J.A., 2010. Ensemble based 4D seismic history matching: Integration of different levels and types of seismic data. In: SPE EUROPEC/EAGE Annual Conference and Exhibition. Society of Petroleum Engineers, <http://dx.doi.org/10.2118/131453-MS>.
- Falcone, G., Gosselin, O., Maire, F., Marraud, J., Zhakupov, M., 2004. Petroelastic modelling as key element of 4D history matching: a field example. In: SPE Annual Technical Conference and Exhibition. Society of Petroleum Engineers, <http://dx.doi.org/10.2118/90466-MS>.
- Fowler, A.M., Dance, S.L., Waller, J.A., 2018. On the interaction of observation and prior error correlations in data assimilation. *Q. J. R. Meteorol. Soc.* 144, 48–62. <http://dx.doi.org/10.1002/qj.3183>.
- Freeze, R.A., 1975. A stochastic-conceptual analysis of one-dimensional groundwater flow in a non-uniform, homogeneous media. *Water Resour. Res.* 11, 725–741. <http://dx.doi.org/10.1029/WR011i005p00725>.
- Furrer, R., Bengtsson, T., 2007. Estimation of high-dimensional prior and posterior covariance matrices in Kalman filter variants. *J. Multivariate Anal.* 98, 227–255. <http://dx.doi.org/10.1016/j.jmva.2006.08.003>.
- Gassmann, F., 1951. Über die Elastizität poröser Medien. *Vierteljahrschrift Naturforschenden Ges.* 96, 1–23.
- Gelman, A., Shalizi, C.R., 2013. Philosophy and the practice of Bayesian statistics. *Br. J. Math. Stat. Psychol.* 66, 8–38. <http://dx.doi.org/10.1111/j.2044-8317.2011.02037.x>.
- Geng, C., MacBeth, C., Chassagne, R., 2017. Seismic history matching using a fast-track simulator to seismic proxy. In: SPE Europec Featured At 79th EAGE Conference and Exhibition. Society of Petroleum Engineers, <http://dx.doi.org/10.2118/185822-MS>.
- van Gestel, J.P., Best, K.D., Barkved, O.I., Kommedal, J.H., 2011. Integration of the life of field seismic data with the reservoir model at the Valhall field. *Geophys. Prospect.* 59, 673–681. <http://dx.doi.org/10.1111/j.1365-2478.2011.00946.x>.
- Gill, C.E., Miotto, A., Floricich, M., Rogers, R., Potter, R.D., Harwijanto, J., Townsley, P., 2012. The Nelson full field model: using iterative quantitative improvements from the initial framework to the final history match. *First Break* 30, 43–53. <http://dx.doi.org/10.3997/1365-2397.2012013>.
- Gosselin, O., Aanonsen, S.I., Aavatsmark, I., Cominelli, A., Gonard, R., Kolasinski, M., Ferdinandi, F., Kovacic, L., Neylon, K., 2003. History matching using time-lapse seismic (HUTS). In: SPE ATCE, 5–8 October, Denver. <http://dx.doi.org/10.2118/84464-MS>.
- Grana, D., Mukerji, T., 2015. Bayesian inversion of time-lapse seismic data for the estimation of static reservoir properties and dynamic property changes. *Geophys. Prospect.* 63, 637–655. <http://dx.doi.org/10.1111/1365-2478.12203>.
- Grana, D., Mukerji, T., Doyen, P., 2021. Seismic Reservoir Modeling: Theory, Examples, and Algorithms. John Wiley & Sons.
- Gu, F., Chan, M., Fryk, R., 2011. Geomechanical-data acquisition, monitoring, and applications in SAGD. *J. Can. Pet. Technol.* 50, 9–21. <http://dx.doi.org/10.2118/145402-PA>.
- Hamill, T.M., Whitaker, J.S., Snyder, C., 2001. Distance-dependent filtering of background error covariance estimates in an ensemble Kalman filter. *Mon. Weather Rev.* 129, 2776–2790. [http://dx.doi.org/10.1175/1520-0493\(2001\)129<2776:DDFOBE>2.0.CO;2](http://dx.doi.org/10.1175/1520-0493(2001)129<2776:DDFOBE>2.0.CO;2).
- Han, G., Vaughn, B., Davids, A., Spokes, J., Newman, R., Adachi, J., 2013. Development and calibrations of a coupled reservoir geomechanics model for Valhall field. In: 47th US Rock Mechanics / Geomechanics Symposium 2013, Vol. 1. pp. 207–215.
- Hashin, Z., Shtrikman, S., 1963. A variational approach to the theory of the elastic behaviour of multiphase materials. *J. Mech. Phys. Solids* 11, 127–140. [http://dx.doi.org/10.1016/0022-5096\(63\)90060-7](http://dx.doi.org/10.1016/0022-5096(63)90060-7).
- Haverl, M., Aga, M., Reiso, E., 2005. Integrated workflow for quantitative use of time-lapse seismic data in history matching: a North Sea field case. In: SPE Europec/EAGE Annual Conference, 13–16 June 2005. Madrid, Spain. <http://dx.doi.org/10.3997/2214-4609-pdb.1.C028>.
- Hetz, G., Kim, H., Datta-Gupta, A., King, M.J., Przybysz-Jarnut, J.K., Lopez, J.L., Vasco, D., 2017. History matching of frequent seismic surveys using seismic onset times at the Peace River Field, Canada. In: SPE Annual Technical Conference and Exhibition. Society of Petroleum Engineers, <http://dx.doi.org/10.2118/187310-MS>.
- Hiebert, A.D., Morrish, I.C., Card, C., Ha, H., Porter, S., Kumar, A., Sun, F., Close, J.C., 2013. Incorporating 4D seismic steam chamber location information into assisted history matching for a SAGD simulation. In: SPE Heavy Oil Conference-Canada, 11–13 June. Calgary, Alberta, Canada. <http://dx.doi.org/10.2118/165420-MS>.
- Hill, R., 1963. Elastic properties of reinforced solids: some theoretical principles. *J. Mech. Phys. Solids* 11, 357–372. [http://dx.doi.org/10.1016/0022-5096\(63\)90036-X](http://dx.doi.org/10.1016/0022-5096(63)90036-X).
- Hodneland, E., Gasda, S., Kaufmann, R., Bekkvik, T.C., Hermanrud, C., Midttømme, K., 2019. Effect of temperature and concentration of impurities in the fluid stream on CO<sub>2</sub> migration in the Utsira formation. *Int. J. Greenh. Gas Control* 83, 20–28. <http://dx.doi.org/10.1016/j.ijggc.2019.01.020>.
- Hosseiniouheri, P., Hosseini, S.A., Nuñez-López, V., Lake, L.W., 2018. Impact of field development strategies on CO<sub>2</sub> trapping mechanisms in a CO<sub>2</sub>-EOR field: A case study in the permian basin (SACROC unit). *Int. J. Greenh. Gas Control* 72, 92–104. <http://dx.doi.org/10.1016/j.ijggc.2018.03.002>.
- Houck, R.T., 2007. Time-lapse seismic repeatability—how much is enough?. *Lead. Edge* 26, 828–834. <http://dx.doi.org/10.1190/1.2756860>.
- Houtekamer, P.L., Mitchell, H.L., 1998. Data assimilation using an ensemble Kalman filter technique. *Mon. Weather Rev.* 126, 796–811. [http://dx.doi.org/10.1175/1520-0493\(1998\)126<0796:DAUAEK>2.0.CO;2](http://dx.doi.org/10.1175/1520-0493(1998)126<0796:DAUAEK>2.0.CO;2).
- Houtekamer, P.L., Mitchell, H.L., 2001. A sequential ensemble Kalman filter for atmospheric data assimilation. *Mon. Weather Rev.* 129, 123–137. [http://dx.doi.org/10.1175/1520-0493\(2001\)129<0123:ASEKFF>2.0.CO;2](http://dx.doi.org/10.1175/1520-0493(2001)129<0123:ASEKFF>2.0.CO;2).
- Hu, L.Y., 2000. Gradual deformation and iterative calibration of gaussian-related stochastic models. *Math. Geol.* 32, 87–108. <http://dx.doi.org/10.1023/A:1007506918588>.

- Hu, L., Le Ravalec, M., Blanc, G., Roggero, F., Noetinger, B., Haas, A., Corre, B., 1999. Reducing uncertainties in production forecasts by constraining geological modeling to dynamic data. In: SPE Annual Technical Conference and Exhibition. Society of Petroleum Engineers, <http://dx.doi.org/10.2118/56703-MS>.
- Huang, X., Meister, L., Workman, R., 1997. Reservoir characterization by integration of time-lapse seismic and production data. In: SPE Annual Technical Conference and Exhibition, 5–8 October. Society of Petroleum Engineers, <http://dx.doi.org/10.2118/38695-MS>.
- Ingber, L., 1989. Very fast simulated re-annealing. *Math. Comput. Modelling* 12, 967–973. [http://dx.doi.org/10.1016/0895-7177\(89\)90202-1](http://dx.doi.org/10.1016/0895-7177(89)90202-1).
- Jin, L., Alpak, F., van den Hoek, P., Pirmez, C., Fehintola, T., Tendo, F., Olaniyan, E., 2012a. A comparison of stochastic data-integration algorithms for the joint history matching of production and time-lapse-seismic data. *SPE Reserv. Eval. Eng.* 15, 498–512. <http://dx.doi.org/10.2118/146418-PA>.
- Jin, L., Weber, D., van den Hoek, P., Alpak, F.O., Pirmez, C., 2012b. 4D seismic history matching using information from the flooded zone. *First Break* 30, <http://dx.doi.org/10.3997/1365-2397.2012011>.
- Kahrobaei, S., van Essen, G.M., Doren, J.F.M.V., den Hof, P.M.J.V., Jansen, J.D., 2013. Adjoint-based history matching of structural models using production and time-lapse seismic data. In: SPE Reservoir Simulation Symposium. Society of Petroleum Engineers, <http://dx.doi.org/10.2118/163586-MS>.
- Kazemi, A., Stephen, K.D., 2012. Schemes for automatic history matching of reservoir modeling: A case of Nelson oilfield in UK. *Pet. Explor. Dev.* 39, 349–361. [http://dx.doi.org/10.1016/S1876-3804\(12\)60051-2](http://dx.doi.org/10.1016/S1876-3804(12)60051-2).
- Kazemi, A., Stephen, K.D., Shams, A., 2011. Seismic history matching of Nelson using time-lapse seismic data: An investigation of 4D signature normalization. *SPE Reserv. Eval. Eng.* 14, 621–633. <http://dx.doi.org/10.2118/131538-PA>.
- Kennedy, M.C., O'Hagan, A., 2001. Bayesian calibration of computer models. *J. R. Stat. Soc. Ser. B Stat. Methodol.* 63, 425–464. <http://dx.doi.org/10.1111/1467-9868.00294>.
- Ketinen, S.P., Kalla, S., Oppert, S., Billiter, T., 2020. Quantitative integration of 4D seismic with reservoir simulation. *SPE J.* 25, 2055–2066. <http://dx.doi.org/10.2118/191521-PA>.
- Kjelstadli, R.M., Lane, H.S., Johnson, D.T., Barkved, O.I., Buer, K., Kristiansen, T.G., 2005. Quantitative history match of 4D seismic response and production data in the Valhall field. In: SPE Offshore Europe Oil and Gas Exhibition and Conference, 6–9 September. Society of Petroleum Engineers, Aberdeen, United Kingdom, <http://dx.doi.org/10.2118/96317-MS>.
- Knight, R., Dvorkin, J., Nur, A., 1998. Acoustic signatures of partial saturation. *Geophysics* 63, 132–138. <http://dx.doi.org/10.1190/1.1444305>.
- Kragh, E., Christie, P., 2002. Seismic repeatability, normalized rms, and predictability. *Lead. Edge* 21, 640–647. <http://dx.doi.org/10.1190/1.1497316>.
- Kretz, V., Vallès, B., Sonneland, L., 2004. Fluid front history matching using 4D seismic and streamline simulation. In: Proceedings of the SPE Annual Technical Conference and Exhibition. Houston, Texas. <http://dx.doi.org/10.2523/90136-ms>.
- Kumar, D., Ahmed, I., 2020. Seismic noise. In: Gupta, H.K. (Ed.), *Encyclopedia of Solid Earth Geophysics*. Springer, Cham, [http://dx.doi.org/10.1007/978-3-030-10475-7\\_146-1](http://dx.doi.org/10.1007/978-3-030-10475-7_146-1).
- Landrø, M., 2001. Discrimination between pressure and fluid saturation changes from time-lapse seismic data. *Geophysics* 66, 836–844. <http://dx.doi.org/10.1190/1.1444973>.
- Landrø, M., Kvam, Ø., 2002. Pore pressure estimation – What can we learn from 4D? *CSEG Rec.* 27, 83–87.
- Larner, K., Chambers, R., Yang, M., Lynn, W., Wai, W., 1983. Coherent noise in marine seismic data. *Geophysics* 48, 854–886. <http://dx.doi.org/10.1190/1.1441516>.
- Le Ravalec, M., Tillier, E., Veiga, S.D., Enchery, G., Gervais, V., 2012. Advanced integrated workflows for incorporating both production and 4D seismic-related data into reservoir models. *Oil Gas Sci. Technol. — Rev. IFP Energ. Nouv.* 67, 207–220. <http://dx.doi.org/10.2516/ogst/2011159>.
- Leeuwenburgh, O., Arts, R., 2014. Distance parameterization for efficient seismic history matching with the ensemble Kalman filter. *Comput. Geosci.* 18, 535–548. <http://dx.doi.org/10.1007/s10596-014-9434-y>.
- Leeuwenburgh, O., Meekes, S., Vandeweyer, V., Brouwer, J., 2016. Stochastic history matching to time-lapse seismic of a CO<sub>2</sub>-EOR project sector model. *Int. J. Greenh. Gas Control* 54, 441–453. <http://dx.doi.org/10.1016/j.ijggc.2016.05.027>.
- Lerat, O., Adjemian, F., Auvinet, A., Baroni, A., Bemmer, E., Eschard, R., Etienne, G., Renard, G., Servant, G., Michel, L., Rodriguez, S., Aubin, F., Euzen, T., 2009. Modelling of 4D seismic data for the monitoring of the steam chamber growth during SAGD process. In: Canadian International Petroleum Conference 2009, CIPC 2009, pp. 21–30. <http://dx.doi.org/10.2118/2009-095>.
- Li, D., Xu, K., Harris, J.M., Darve, E., 2020. Coupled time-lapse full-waveform inversion for subsurface flow problems using intrusive automatic differentiation. *Water Resour. Res.* <http://dx.doi.org/10.1029/2019WR027032>.
- Liu, T., Chen, H., Hetz, G., Datta-Gupta, A., 2020. Integration of time-lapse seismic data using the onset time approach: The impact of seismic survey frequency. *J. Pet. Sci. Eng.* 189, <http://dx.doi.org/10.1016/j.petrol.2020.106989>.
- Liu, M., Grana, D., 2019. Time-lapse seismic history matching with iterative ensemble smoother and deep convolutional autoencoder. *Geophysics* 85, 1–63. <http://dx.doi.org/10.1190/geo2019-0019.1>.
- Liu, N., Oliver, D.S., 2004. Experimental assessment of gradual deformation method. *Math. Geol.* 36, 65–77. <http://dx.doi.org/10.1023/B:MATG.0000016230.52968.6e>.
- Liu, Z.Q., Rabier, F., 2002. The interaction between model resolution, observation resolution and observation density in data assimilation: A one-dimensional study. *Q. J. R. Meteorol. Soc.* 128, 1367–1386. <http://dx.doi.org/10.1256/003590002320373337>.
- Lorentzen, R.J., Bhakta, T., Grana, D., Luo, X., Valestrand, R., Nævdal, G., 2020. Simultaneous assimilation of production and seismic data: application to the Norne field. *Comput. Geosci.* 24, 907–920. <http://dx.doi.org/10.1007/s10596-019-09900-0>.
- Lorentzen, R.J., Luo, X., Bhakta, T., Valestrand, R., 2019. History matching the full Norne Field model using seismic and production data. *SPE J.* 24, 1452–1467. <http://dx.doi.org/10.2118/194205-PA>.
- Lu, M., Chen, Y., 2020. Improved estimation and forecasting through residual-based model error quantification. *SPE J.* 25, 951–968. <http://dx.doi.org/10.2118/199358-PA>.
- Luo, X., Bhakta, T., 2017. Estimating observation error covariance matrix of seismic data from a perspective of image denoising. *Comput. Geosci.* 21, 205–222. <http://dx.doi.org/10.1007/s10596-016-9605-0>.
- Luo, X., Bhakta, T., Jakobsen, M., Nævdal, G., 2017. An ensemble 4D-seismic history-matching framework with sparse representation based on wavelet multiresolution analysis. *SPE J.* 22, 985–1010. <http://dx.doi.org/10.2118/180025-PA>.
- Luo, X., Bhakta, T., Jakobsen, M., Nævdal, G., 2018a. Efficient big data assimilation through sparse representation: A 3D benchmark case study in petroleum engineering. *PLOS ONE* 13, e0198586. <http://dx.doi.org/10.1371/journal.pone.0198586>.
- Luo, X., Bhakta, T., Nævdal, G., 2018b. Correlation-based adaptive localization with applications to ensemble-based 4D seismic history matching. *SPE J.* 23, <http://dx.doi.org/10.2118/185936-PA>.
- Luo, X., Stordal, A.S., Lorentzen, R.J., Nævdal, G., 2015. Iterative ensemble smoother as an approximate solution to a regularized minimum-average-cost problem: Theory and applications. *SPE J.* 20, 962–982. <http://dx.doi.org/10.2118/176023-PA>.
- Lygren, M., Husby, O., Osdal, B., El Ouair, Y., Springer, M., 2005. History matching using 4D seismic and pressure data on the Norne field. In: 67th EAGE Conference & Exhibition. <http://dx.doi.org/10.3997/2214-4609-pdb.1.C003>.
- MacBeth, C., 2004. A classification for the pressure-sensitivity properties of a sandstone rock frame. *Geophysics* 69, 497–510. <http://dx.doi.org/10.1190/1.1707070>.
- MacBeth, C., Geng, C., Chassagne, R., 2016. A fast-track simulator to seismic proxy for quantitative 4D seismic analysis. In: SEG Technical Program Expanded Abstracts 2016. Society of Exploration Geophysicists, pp. 5537–5541. <http://dx.doi.org/10.1190/segam2016-13818132.1>.
- Madsen, R.B., Hansen, T.M., 2018. Estimation and accounting for the modeling error in probabilistic linearized amplitude variation with offset inversion. *Geophysics* 83, N15–N30. <http://dx.doi.org/10.1190/geo2017-0404.1>.
- Maleki, M., Davolio, A., Schiozer, D.J., 2018. Using simulation and production data to resolve ambiguity in interpreting 4D seismic inverted impedance in the Norne Field. *Pet. Geosci.* 24, 335–347. <http://dx.doi.org/10.1144/petgeo2017-032>.
- Maleki, M., Davolio, A., Schiozer, D.J., 2019. Quantitative integration of 3D and 4D seismic impedance into reservoir simulation model updating in the Norne Field. *Geophys. Prospect.* 67, 167–187. <http://dx.doi.org/10.1111/1365-2478.12717>.
- Mannseth, T., Fossum, K., 2018. Assimilating spatially dense data for subsurface applications – balancing information and degrees of freedom. *Comput. Geosci.* 22, 1323–1349. <http://dx.doi.org/10.1007/s10596-018-9755-3>.
- Marsily, G., Lavedan, G., Boucher, M., Fasanino, G., 1984. Interpretation of interference tests in a well field using geostatistical techniques to fit the permeability distribution in a reservoir model. In: *Geostatistics for Natural Resources Characterization*. Springer Netherlands, Dordrecht, pp. 831–849. [http://dx.doi.org/10.1007/978-94-009-3701-7\\_16](http://dx.doi.org/10.1007/978-94-009-3701-7_16).
- Maschio, C., Schiozer, D.J., 2016. Probabilistic history matching using discrete Latin Hypercube sampling and nonparametric density estimation. *J. Pet. Sci. Eng.* 147, 98–115. <http://dx.doi.org/10.1016/j.petrol.2016.05.011>.
- Mavko, G., Mukerji, T., Dvorkin, J., 2009. *The Rock Physics Handbook: Tools for Seismic Analysis of Porous Media*. Cambridge University Press, <http://dx.doi.org/10.1017/CBO9780511626753>.
- Menezes, C.A., Gosselin, O.R., 2006. From logs scale to reservoir scale: Upscaling of the petro-elastic model. In: SPE Europe/EAGE Annual Conference and Exhibition. Society of Petroleum Engineers, <http://dx.doi.org/10.2118/100233-MS>.
- Mitchell, P., Chassagne, R., 2019. 4D assisted seismic history matching using a differential evolution algorithm at the Harding South Field. In: 81st EAGE Conference and Exhibition. European Association of Geoscientists & Engineers, <http://dx.doi.org/10.3997/2214-4609.201901216>.
- de Moraes, R.J., Hajibeygi, H., Jansen, J.D., 2020. A multiscale method for data assimilation. *Comput. Geosci.* 24, 425–442. <http://dx.doi.org/10.1007/s10596-019-09839-2>.
- de Moraes, R.J., Rodrigues, J.R.P., Hajibeygi, H., Jansen, J.D., 2018. Computing derivative information of sequentially coupled subsurface models. *Comput. Geosci.* 22, 1527–1541. <http://dx.doi.org/10.1007/s10596-018-9772-2>.
- Nes, O.M., Holt, R.M., Fjaer, E., 2002. The reliability of core data as input to seismic reservoir monitoring studies. *SPE Reserv. Eval. Eng.* 5, 79–86. <http://dx.doi.org/10.2118/76641-PA>.

- Nivlet, P., Smith, R., Jervis, M.A., Bakulin, A., 2017. Toward an integrated and realistic interpretation of continuous 4D seismic data for a CO<sub>2</sub> EOR and sequestration project. In: SPE Middle East Oil & Gas Show and Conference, 6–9 March. Society of Petroleum Engineers, Manama, Kingdom of Bahrain, <http://dx.doi.org/10.2118/183789-MS>.
- da Nobrega, D.V., de Moraes, F.S., Emerick, A.A., 2018. Data assimilation of a legacy 4D seismic in a brown field. *J. Geophys. Eng.* 15, 2585–2601. <http://dx.doi.org/10.1088/1742-2140/aadd68>.
- Obidegwu, D., Chassagne, R., MacBeth, C., 2017. Seismic assisted history matching using binary maps. *J. Nat. Gas Sci. Eng.* 42, <http://dx.doi.org/10.1016/j.jngse.2017.03.001>.
- Oliver, D.S., 2020. Diagnosing reservoir model deficiency for model improvement. *J. Pet. Sci. Eng.* 193, 107367. <http://dx.doi.org/10.1016/j.petrol.2020.107367>.
- Oliver, D.S., Alfonzo, M., 2018. Calibration of imperfect models to biased observations. *Comput. Geosci.* 22, 145–161. <http://dx.doi.org/10.1007/s10596-017-9678-4>.
- Oliver, D.S., Chen, Y., 2011. Recent progress on reservoir history matching: a review. *Comput. Geosci.* 15, 185–221. <http://dx.doi.org/10.1007/s10596-010-9194-2>.
- Oliver, D.S., Reynolds, A.C., Liu, N., 2008. Inverse Theory for Petroleum Reservoir Characterization and History Matching. Cambridge University Press, <http://dx.doi.org/10.1017/CBO9780511535642>.
- Omofofoma, V.E., MacBeth, C., 2016. Quantification of reservoir pressure-sensitivity using multiple monitor 4D seismic data. In: 78th EAGE Conference and Exhibition 2016, European Association of Geoscientists & Engineers. pp. 1–5. <http://dx.doi.org/10.3997/2214-4609.201601315>.
- Osdal, B., Haverl, M., 2019. 4D AVO analysis for pressure and water flooding discrimination on Norne Field. In: 81st EAGE Conference and Exhibition 2019, June 2019. European Association of Geoscientists & Engineers, pp. 1–5. <http://dx.doi.org/10.3997/2214-4609.201901212>.
- Osdal, B., Husby, O., Aronsen, H.A., Chen, N., Alsos, T., 2006. Mapping the fluid front and pressure buildup using 4D data on Norne Field. *Lead. Edge* 25, 1134–1141. <http://dx.doi.org/10.1190/1.2349818>.
- Ouenes, A., Anderson, T.C., Klepacki, D., Bachir, A., Boukhelf, D., Robinson, G.C., Holmes, M., Black, B.J., Stamp, V.W., 2010. Integrated characterization and simulation of the fractured Tensleep Reservoir at Teapot Dome for CO<sub>2</sub> injection design. In: SPE Western Regional Meeting, Society of Petroleum Engineers. pp. 135–149. <http://dx.doi.org/10.2118/132404-MS>.
- Pamukcu, Y., Hurter, S., Jammes, L., Vu-Hoang, D., Pekot, L., 2011. Characterizing and predicting short term performance for the In Salah Krecbba field CCS joint industry project. *Energy Procedia* 3371–3378. <http://dx.doi.org/10.1016/j.egypro.2011.02.259>.
- Park, H.Y., Datta-Gupta, A., King, M.J., 2015. Handling conflicting multiple objectives using Pareto-based evolutionary algorithm during history matching of reservoir performance. *J. Pet. Sci. Eng.* 125, 48–66. <http://dx.doi.org/10.1016/j.petrol.2014.11.006>.
- Peaceman, D.W., 1977. *Fundamentals of Numerical Reservoir Simulation*. Elsevier scientific publishing company.
- Powell, M.J.D., 1968. A Fortran Subroutine for Solving Systems of Nonlinear Algebraic Equations. Technical Report, Theoretical Physics Division, Atomic Energy Research Establishment, Harwell, Berkshire.
- Raanes, P.N., Stordal, A.S., Evensen, G., 2019. Revising the stochastic iterative ensemble smoother. *Nonlinear Process. Geophys.* 26, 325–338. <http://dx.doi.org/10.5194/npg-26-325-2019>.
- Reuss, A., 1929. Berechnung der fließgrenze von mischkristallen auf grund der plastizitätsbedingung für einkristalle. *ZAMM-J. Appl. Math. Mech./Z. Angew. Math. Mech.* 9, 49–58. <http://dx.doi.org/10.1002/Zamm.1929009104>.
- Reynolds, A.C., Zafari, M., Li, G., 2006. Iterative forms of the ensemble Kalman filter. In: Proceedings of 10th European Conference on the Mathematics of Oil Recovery. European Association of Geoscientists & Engineers, Amsterdam, The Netherlands, <http://dx.doi.org/10.3997/2214-4609.201402496>.
- Roach, L.A.N., White, D.J., Roberts, B., 2015. Assessment of 4D seismic repeatability and CO<sub>2</sub> detection limits using a sparse permanent land array at the Aquistore CO<sub>2</sub> storage site. *Geophysics* 80, WA1–WA13. <http://dx.doi.org/10.1190/geo2014-0201.1>.
- Robinson, E.A., Durrani, T.S., Peardon, L.G., 1986. *Geophysical Signal Processing*. Prentice-Hall, Inc..
- Roggero, F., Ding, D.Y., Berthet, P., Lerat, O., Cap, J., Schreiber, P.E., 2007. Matching of production history and 4D seismic data—application to the Girassol Field, Offshore Angola. In: SPE Annual Technical Conference and Exhibition. Society of Petroleum Engineers, <http://dx.doi.org/10.2118/109929-MS>.
- Roggero, F., Hu, L., 1998. Gradual deformation of continuous geostatistical models for history matching. In: SPE Annual Technical Conference and Exhibition. Society of Petroleum Engineers, <http://dx.doi.org/10.2118/49004-MS>.
- Roggero, F., Lerat, O., Ding, D.Y., Berthet, P., Bordenave, C., Lefeuvre, F., Perfetti, P., 2012. History matching of production and 4D seismic data: Application to the Girassol Field, Offshore Angola. *Oil Gas Sci. Technol. — Rev. IFP Energ. Nouv.* 67, 237–262. <http://dx.doi.org/10.2516/ogst/2011148>.
- Rwechungura, R.W., Suwartadi, E., Dadashpour, M., Kleppe, J., Foss, B.A., 2010. The Norne Field case – a unique comparative case study. In: SPE Intelligent Energy Conference and Exhibition. Society of Petroleum Engineers, <http://dx.doi.org/10.2118/127538-MS>.
- Sagitov, I., Stephen, K.D., 2012. Assisted seismic history matching in different domains - what seismic data should we compare? In: 74th EAGE Conference and Exhibition Incorporating EUROPEC 2012. European Association of Geoscientists & Engineers, pp. pp–293. <http://dx.doi.org/10.2118/154503-MS>.
- Sagitov, I., Stephen, K.D., 2013. Optimizing the integration of 4D seismic data in history matching: Which data should we compare? In: EAGE Annual Conference & Exhibition Incorporating SPE Europec, London, 10–13 June. Society of Petroleum Engineers, <http://dx.doi.org/10.2118/164852-MS>.
- Sambridge, M., 1999. Geophysical inversion with a neighbourhood algorithm - I. Searching a parameter space. *Geophys. J. Int.* 138, 479–494. <http://dx.doi.org/10.1046/j.1365-246X.1999.00876.x>.
- Santos, J.M.C.d., Davolio, A., Schiozer, D.J., MacBeth, C., 2018. Semiquantitative 4D seismic interpretation integrated with reservoir simulation: Application to the Norne field. *Interpretation* 6, T601–T611. <http://dx.doi.org/10.1190/INT-2017-0122.1>.
- Sedighi, F., Stephen, K.D., 2010. Faster convergence in seismic history matching by dividing and conquering the unknowns. *SPE J.* 15, 1083–1094. <http://dx.doi.org/10.2118/121210-PA>.
- Shi, J.Q., Durucan, S., Korre, A., Ringrose, P., Mathieson, A., 2019. History matching and pressure analysis with stress-dependent permeability using the In Salah CO<sub>2</sub> storage case study. *Int. J. Greenh. Gas Control* 91, <http://dx.doi.org/10.1016/j.ijggc.2019.102844>.
- Shokri, A.R., Chalaturnyk, R.J., Nickel, E., 2019. Non-isothermal injectivity considerations for effective geological storage of CO<sub>2</sub> at the Aquistore site, Saskatchewan, Canada. In: Proceedings - SPE Annual Technical Conference and Exhibition 2019-Septe. <http://dx.doi.org/10.2118/196118-MS>.
- Singh, V.P., Cavanagh, A., Hansen, H., Nazarian, B., Iding, M., Ringrose, P.S., 2010. Reservoir modeling of CO<sub>2</sub> plume behavior calibrated against monitoring data from Sleipner, Norway. In: SPE Annual Technical Conference and Exhibition. Society of Petroleum Engineers, pp. 3461–3479. <http://dx.doi.org/10.2118/134891-MS>.
- Skjervheim, J.A., Evensen, G., Aanonsen, S.I., Ruud, B.O., Johansen, T.A., 2007. Incorporating 4D seismic data in reservoir simulation models using ensemble Kalman filter. *SPE J.* 12, 282–292. <http://dx.doi.org/10.2118/95789-MS>.
- Skjervheim, J.A., Evensen, G., Hove, J., Vabø, J.G., 2011. An ensemble smoother for assisted history matching. In: SPE Reservoir Simulation Symposium. The Woodlands, Texas, USA. <http://dx.doi.org/10.2118/141929-MS>.
- Smith, B.A., Sylte, J.E., Clausen, C.K., Guilbot, J., 2002. Ekofisk 4D seismic - Influence on flow simulation and compaction modeling. In: Proceedings of the Annual Offshore Technology Conference. <http://dx.doi.org/10.4043/14149-MS>.
- Soares, R.V., Luo, X., Evensen, G., 2019. Sparse representation of 4D seismic signal based on dictionary learning. In: SPE Norway One Day Seminar. Society of Petroleum Engineers, <http://dx.doi.org/10.2118/195599-MS>.
- Soares, R., Luo, X., Evensen, G., Bhakta, T., 2020. 4D seismic history matching: Assessing the use of a dictionary learning based sparse representation method. *J. Pet. Sci. Eng.* 195, 107763. <http://dx.doi.org/10.1016/j.petrol.2020.107763>.
- Souza, R., Lumley, D., Shragge, J., 2017. Estimation of reservoir fluid saturation from 4D seismic data: effects of noise on seismic amplitude and impedance attributes. *J. Geophys. Eng.* 14, 51–68. <http://dx.doi.org/10.1088/1742-2132/14/1/51>.
- Souza, R., Lumley, D., Shragge, J., Davolio, A., Schiozer, D.J., 2018. Analysis of time-lapse seismic and production data for reservoir model classification and assessment. *J. Geophys. Eng.* 15, 1561–1587. <http://dx.doi.org/10.1088/1742-2140/aab287>.
- Souza, R.M., Machado, A.F., Munerato, F.P., Schiozer, D.J., 2010. Iterative history matching technique for estimating reservoir parameters from seismic data. In: SPE EUROPEC/EAGE Annual Conference and Exhibition. Society of Petroleum Engineers, <http://dx.doi.org/10.2118/131617-MS>.
- Stephen, K.D., 2007. Scale and process dependent model errors in seismic history matching. *Oil Gas Sci. Technol.* 62, 123–135. <http://dx.doi.org/10.2516/ogst:2007011>.
- Stephen, K.D., 2018. Assisted seismic history matching of the Nelson field: Managing large numbers of unknowns by divide and conquer. *J. Pet. Sci. Eng.* 171, 1232–1248. <http://dx.doi.org/10.1016/j.petrol.2018.07.055>.
- Stephen, K.D., Kazemi, A., 2014. Improved normalization of time-lapse seismic data using normalized root mean square repeatability data to improve automatic production and seismic history matching in the Nelson field. *Geophys. Prospect.* 62, 1009–1027. <http://dx.doi.org/10.1111/1365-2478.12109>.
- Stephen, K.D., MacBeth, C., 2008. Reducing reservoir prediction uncertainty by updating a stochastic model using seismic history matching. *SPE Reserv. Eval. Eng.* 11, 991–999. <http://dx.doi.org/10.2118/100295-PA>.
- Stephen, K.D., Shams, A., MacBeth, C., 2009. Faster seismic history matching in a United Kingdom continental shelf reservoir. *SPE Reserv. Eval. Eng.* 12, 586–594. <http://dx.doi.org/10.2118/107147-PA>.
- Stephen, K.D., Soldo, J., MacBeth, C., Christie, M., 2006. Multiple-model seismic and production history matching: A case study. *SPE J.* 11, 418–430. <http://dx.doi.org/10.2118/94173-PA>.
- Stewart, L.M., Dance, S.L., Nichols, N.K., 2008. Correlated observation errors in data assimilation. *Internat. J. Numer. Methods Fluids* 56, 1521–1527. <http://dx.doi.org/10.1002/fld.1636>.
- Suman, A., Mukerji, T., 2013. Sensitivity study of rock-physics parameters for modeling time-lapse seismic response of Norne field. *Geophysics* 78, D511–D523. <http://dx.doi.org/10.1190/geo2013-0045.1>.

- Sun, W., Vink, J.C., Gao, G., 2017. A practical method to mitigate spurious uncertainty reduction in history matching workflows with imperfect reservoir models. In: SPE Reser. Simul. Conf. 20–22 February, Texas. <http://dx.doi.org/10.2118/182599-MS>.
- Tarantola, A., 1984. Inversion of seismic reflection data in the acoustic approximation. *Geophysics* 49, 1259–1266. <http://dx.doi.org/10.1190/1.1441754>.
- Tarantola, A., 2005. Inverse Problem Theory and Methods for Model Parameter Estimation. SIAM, <http://dx.doi.org/10.1137/1.9780898717921>.
- Thore, P., 2015. Uncertainty in seismic inversion: What really matters? *Lead. Edge* 34, 1000–1004. <http://dx.doi.org/10.1190/1.1190/1.1441754>.
- Tillier, E., Da Veiga, S., Derfoul, R., 2013. Appropriate formulation of the objective function for the history matching of seismic attributes. *Comput. Geosci.* 51, 64–73.
- Tolstukhin, E., Hu, L.Y., Sudan, H.H., 2014. Geologically consistent seismic history matching workflow for Ekofisk Chalk Reservoir. In: ECMOR XIV – 14th European Conference on the Mathematics of Oil Recovery, 2014. European Association of Geoscientists & Engineers, <http://dx.doi.org/10.3997/2214-4609.20141781>.
- Tolstukhin, E., Lyngnes, B., Sudan, H.H., 2012. Ekofisk 4D seismic—seismic history matching workflow. In: SPE Europec/EAGE Annual Conference, Copenhagen, 4–7 June. <http://dx.doi.org/10.2118/154347-MS>.
- Trani, M., Arts, R., Leeuwenburgh, O., 2012. Seismic history matching of fluid fronts using the ensemble Kalman filter. *SPE J.* 18, 159–171. <http://dx.doi.org/10.2118/163043-PA>.
- Trani, M., Wojnar, K., Moncorgé, A., Philippe, B., 2017. Ensemble-based assisted history matching using 4D seismic fluid front parameterization. In: SPE Middle East Oil and Gas Show and Conference, MEOS, Proceedings. pp. 640–652. <http://dx.doi.org/10.2118/183901-ms>.
- Vasco, D.W., Bakulin, A., Baek, H., Johnson, L.R., 2015. Reservoir characterization based upon the onset of time-lapse amplitude changes. *Geophysics* 80, M1–M14. <http://dx.doi.org/10.1190/geo2014-0076.1>.
- Vasco, D., Daley, T.M., Bakulin, A., 2014. Utilizing the onset of time-lapse changes: A robust basis for reservoir monitoring and characterization. *Geophys. J. Int.* 197, 542–556. <http://dx.doi.org/10.1093/gji/ggt526>.
- Vedanti, N., Sen, M.K., 2009. Seismic inversion tracks in situ combustion: A case study from Balol oil field, India. *Geophysics* 74, <http://dx.doi.org/10.1190/1.3129262>.
- Vink, J.C., Gao, G., Chen, C., 2015. Bayesian style history matching: Another way to under-estimate forecast uncertainty?. In: SPE Annual Technical Conference and Exhibition. Society of Petroleum Engineers, <http://dx.doi.org/10.2118/175121-MS>.
- Virieux, J., Asnaashari, A., Brossier, R., Métivier, L., Ribodetti, A., Zhou, W., 2017. An introduction to full waveform inversion. In: Grechka, V., Wapenaar, K. (Eds.), *Encyclopedia of Exploration Geophysics*. In: Geophysical References Series, Society of Exploration Geophysicists, pp. R1–R1–40. <http://dx.doi.org/10.1190/1.9781560803027.entry6>.
- Voigt, W., 1929. *Lehrbuch der Kristallphysik*. BG Teubner Verlag.
- Volkov, O., Bukshynov, V., Durlafsky, L.J., Aziz, K., 2018. Gradient-based Pareto optimal history matching for noisy data of multiple types. *Comput. Geosci.* 22, 1465–1485. <http://dx.doi.org/10.1007/s10596-018-9766-0>.
- Waggoner, J.R., Cominelli, A., Seymour, R.H., Stradiotti, A., 2003. Improved reservoir modelling with time-lapse seismic data in a Gulf of Mexico gas condensate reservoir. *Pet. Geosci.* 9, 61–72. <http://dx.doi.org/10.1144/1354-079302-512>.
- Walker, G.J., Lane, H.S., 2007. Assessing the accuracy of history-match predictions and the impact of time-lapse seismic data: A case study for the Harding reservoir. In: SPE Reservoir Simulation Symposium, Houston, Texas, 26–28 February. Society of Petroleum Engineers, <http://dx.doi.org/10.2118/106019-MS>.
- Watanabe, S., Han, J., Hetz, G., Datta-Gupta, A., King, M.J., Vasco, D.W., 2017. Streamline-based time-lapse-seismic-data integration incorporating pressure and saturation effects. *SPE J.* 22, 1261–1279. <http://dx.doi.org/10.2118/166395-PA>.
- White, R.E., Simm, R., 2003. Tutorial: Good practice in well ties. *First Break* 21, <http://dx.doi.org/10.3997/1365-2397.21.10.25640>.
- Williams, G.A., Chadwick, R.A., 2017. An improved history-match for layer spreading within the Sleipner plume including thermal propagation effects. *Energy Procedia* 114, 2856–2870. <http://dx.doi.org/10.1016/j.egypro.2017.03.1406>, 13th International Conference on Greenhouse Gas Control Technologies, GHGT-13, 14–18 November 2016, Lausanne, Switzerland.
- Yin, Z., Ayzenberg, M., MacBeth, C., Feng, T., Chassagne, R., 2015. Enhancement of dynamic reservoir interpretation by correlating multiple 4D seismic monitors to well behavior. *Interpret.-J. Subsurf. Charact.* 3, SP35–SP52. <http://dx.doi.org/10.1190/INT-2014-0194.1>.
- Yin, Z., Feng, T., MacBeth, C., 2019. Fast assimilation of frequently acquired 4D seismic data for reservoir history matching. *Comput. Geosci.* 128, 30–40. <http://dx.doi.org/10.1016/j.cageo.2019.04.001>.
- Zhang, Y., Leeuwenburgh, O., 2017. Image-oriented distance parameterization for ensemble-based seismic history matching. *Comput. Geosci.* 21, 713–731. <http://dx.doi.org/10.1007/s10596-017-9652-1>.
- Zhang, G., Lu, P., Zhu, C., 2014. Model predictions via history matching of CO<sub>2</sub> plume migration at the Sleipner project, Norwegian North Sea. *Energy Procedia* 3000–3011. <http://dx.doi.org/10.1016/j.egypro.2014.11.323>.
- Zhao, Y., Li, G., Reynolds, A.C., 2007. Characterization of the measurement error in time-lapse seismic data and production data with an EM algorithm. *Oil Gas Sci. Technol.* 62, 181–193. <http://dx.doi.org/10.2516/ogst:2007016>.
- Zhu, C., Zhang, G., Lu, P., Meng, L., Ji, X., 2015. Benchmark modeling of the Sleipner CO<sub>2</sub> plume: Calibration to seismic data for the uppermost layer and model sensitivity analysis. *Int. J. Greenh. Gas Control* 43, 233–246. <http://dx.doi.org/10.1016/j.ijggc.2014.12.016>.